

Deconfining Phase Transition as a Matrix Model of Renormalized Polyakov Loops

Adrian Dumitru,^a Yoshitaka Hatta,^{b,c,d} Jonathan Lenaghan,^e Kostas Orginos,^{f,g} and Robert D. Pisarski^{d,h}

^a*Institut für Theoretische Physik, J. W. Goethe Univ.,
Postfach 11 19 32, 60054 Frankfurt, Germany*

^b*Department of Physics,
Kyoto University, Kyoto 606-8502, Japan*

^c*The Institute of Physical and Chemical Research (RIKEN) Wako,
Saitama 351-0198, Japan*

^d*High Energy Theory, Dept. of Physics,
Brookhaven National Lab., Upton, NY, 11973, U.S.A.*

^e*Dept. of Physics, Univ. of Virginia,
Charlottesville, VA, 22904, U.S.A.*

^f*RIKEN/BNL, Dept. of Physics,
Brookhaven National Lab., Upton, N.Y., 11973, U.S.A.*

^g*Center for Theoretical Physics,
Laboratory for Nuclear Science and Department of Physics,
Massachusetts Institute of Technology,
Cambridge, MA 02139-4307*

^h*Niels Bohr Institute, Blegdamsvej 17,
2100 Copenhagen, Denmark*

(Dated: October 9, 2018)

We discuss how to extract renormalized from bare Polyakov loops in $SU(N)$ lattice gauge theories at nonzero temperature. Single loops in an irreducible representation are multiplicatively renormalized, without mixing, through mass renormalization. The values of renormalized loops in the four lowest representations of $SU(3)$ were measured numerically on small, coarse lattices. We find that in magnitude, condensates for the sextet and octet loops are approximately the square of the triplet loop. This agrees with a large N expansion, where factorization implies that the expectation values of loops in adjoint and higher representations are powers of fundamental and anti-fundamental loops. The corrections to the large N relations at three colors are greatest for the sextet loop, $\sim 1/N$, and are found to be $\leq 25\%$. The values of the renormalized triplet loop can be described by a matrix model, with an effective action dominated by the triplet loop: the deconfining phase transition for $N = 3$ is close to the Gross–Witten point at $N = \infty$.

PACS numbers:

I. INTRODUCTION

In a $SU(N)$ gauge theory, 't Hooft showed that the exact order parameter for deconfinement is a global $Z(N)$ spin [1, 2, 3, 4, 5, 6, 7, 8, 9, 10, 11, 12, 13, 14, 15, 16, 17, 18, 19, 20, 21, 22, 23]. The global $Z(N)$ symmetry arises topologically [12] from the center of the gauge group, and is exact in a pure gauge theory. Quarks carry $Z(N)$ charge, and so break the gluonic $Z(N)$ symmetry. Nevertheless, numerical results from the lattice, termed flavor independence [24], suggest that the gluonic $Z(3)$ symmetry may be an approximate symmetry of QCD .

At a nonzero temperature T , a gluonic $Z(N)$ spin is constructed by starting with a thermal Wilson line, which wraps all of the way around in imaginary time. The trace of the thermal Wilson line is the Polyakov loop [2],

$$\ell_N = \frac{1}{N} \text{tr } \mathbf{L}_N, \quad (1)$$

and is gauge invariant. This is the trace of the propagator for an infinitely massive, test quark; the subscripts denote that the test quark is in the fundamental representation, of dimension N .

As a gauge theory is heated, deconfinement occurs above a temperature T_d . The confined phase is $Z(N)$ symmetric, so the expectation value of the fundamental loop, which has unit $Z(N)$ charge, vanishes below T_d . The gluon spin condenses in the deconfined phase, above T_d :

$$\langle \ell_N \rangle = e^{i\phi} |\langle \ell_N \rangle| \neq 0, \quad e^{i\phi N} = 1, \quad T > T_d, \quad (2)$$

and thereby breaks the global $Z(N)$ symmetry spontaneously [1, 2, 3, 4, 5, 6, 7, 8, 9, 10, 11, 12, 13, 14, 15, 16, 17, 18, 19, 20, 21, 22, 23].

To compute near T_d , it is necessary to employ numerical simulations on the lattice [24, 25, 26, 27, 28, 29, 30]. The difficulty is that the expectation value of the Polyakov loop is a bare quantity, and so suffers ultraviolet divergences. This is due to an additive mass shift which the test quark undergoes with a lattice regularization. In four spacetime dimensions, the mass divergence for a test quark is linear in the ultraviolet cutoff, proportional to the inverse of the lattice spacing, a . This mass renormalization affects the expectation value of the bare Polyakov loop as the exponential of a divergent mass, m_N^{div} , times

the length of the path [31, 32, 33, 34, 35, 36, 37]:

$$|\langle \ell_N \rangle| \sim \exp\left(-\frac{m_N^{div}}{T}\right) \quad , \quad m_N^{div} \sim \frac{1}{a} . \quad (3)$$

For a Polyakov loop, the length of the path is $1/T$.

Gervais and Neveu [31], Polyakov [32], and others [33, 34, 35, 36, 37] established that Wilson lines are renormalizable operators. We review these results in sec. II, applying them to $\ell_{\mathcal{R}}$, a single Polyakov loop in an arbitrary, irreducible representation, \mathcal{R} . A renormalized loop, $\tilde{\ell}_{\mathcal{R}}$, is formed by dividing the bare loop by the appropriate renormalization constant, $\mathcal{Z}_{\mathcal{R}}$:

$$\tilde{\ell}_{\mathcal{R}} = \frac{1}{\mathcal{Z}_{\mathcal{R}}} \ell_{\mathcal{R}} \quad , \quad \mathcal{Z}_{\mathcal{R}} = \exp\left(-\frac{m_{\mathcal{R}}^{div}}{T}\right) . \quad (4)$$

This is a standard type of mass renormalization [38]; for example, in perturbation theory $am_{\mathcal{R}}^{div}$ is a power series in the coupling constant. The only unusual feature is that because the Wilson line is a nonlocal operator, the renormalization constant depends upon the length of the path; in general, the renormalization constant for a path of length \mathcal{L} is $\mathcal{Z}_{\mathcal{R}} = \exp(-m_{\mathcal{R}}^{div}\mathcal{L})$.

The real problem is how to extract the divergent masses non-perturbatively. In this paper we suggest a way of doing this. Consider a set of lattices, all at the same physical temperature, T , but with different values of the lattice spacing, a . Since the number of time steps, $N_t = 1/(aT)$, changes between these lattices, the divergent mass, $am_{\mathcal{R}}^{div}$, follows by comparing the values of the bare Polyakov loops. This assumes that, as in perturbation theory, $am_{\mathcal{R}}^{div}$ is a function only of the temperature, and not of the lattice spacing, as $a \rightarrow 0$. Given the renormalization constant $\mathcal{Z}_{\mathcal{R}}$, the renormalized loop $\tilde{\ell}_{\mathcal{R}}$ then follows from (4), up to corrections at finite lattice spacing $\sim aT$.

In an asymptotically free theory, at high temperature the vacuum is trivial in perturbation theory, as the thermal Wilson line is a $Z(N)$ phase times the unit matrix, $\mathbf{L}_N \rightarrow e^{i\phi} \mathbf{1}_N$ (2). After suitable normalization, the expectation value of any renormalized loop approaches one at high temperature,

$$\left| \langle \tilde{\ell}_{\mathcal{R}} \rangle \right| \rightarrow 1 \quad , \quad T \rightarrow \infty . \quad (5)$$

In sec. III we present measurements of bare and renormalized loops obtained through numerical simulations in a pure $SU(3)$ lattice gauge theory. Polyakov loops in the four lowest representations were measured, although we only found significant signals for three: the fundamental, the symmetric two-index tensor, and the adjoint representations. For three colors, these are the triplet, the sextet, and the octet representations, respectively. These loops were measured at temperatures from $\approx .5T_d \rightarrow 3T_d$. Numerically, we find that in all representations, the divergent masses $am_{\mathcal{R}}^{div}$ are positive, so the bare loops vanish in the continuum limit, $N_t \rightarrow \infty$.

The values of renormalized loops appear to have a well-defined continuum limit and approximately satisfy the asymptotic condition of (5).

An alternate procedure for computing the renormalized Polyakov loop was developed by Kaczmarek, Karsch, Petreczky, and Zantow [39]. They obtain $\mathcal{Z}_{\mathcal{R}}$ from the two point function of Polyakov loops at short distances. Their numerical values for the triplet Polyakov loop agree with ours at T_d , but differ at higher temperatures; they did not consider higher representations.

The most basic thing to consider is the size of the renormalized triplet loop. As we shall see, loops in higher representations are approximately given as powers of the triplet loop. We define a perturbative regime when the expectation value of the renormalized triplet loop is near one in magnitude. If the triplet loop is nonzero, but not close to one, then we have a deconfined, but non-perturbative, regime. At the transition, $T = T_d^+$, both we and Kaczmarek *et al.* [39] find that the renormalized triplet loop, $|\langle \tilde{\ell}_3 \rangle|$, is $\approx .4$; by $\approx 3T_d$, we find it is $\approx .9$, while [39] finds ≈ 1.0 . This suggests that a pure gauge theory is, in some sense, perturbative from temperatures of $\approx 3T_d$ on up, but not from T_d to $\approx 3T_d$. This is in qualitative agreement with different resummations of perturbation theory [7], all of which work down only to a temperature which is several times T_d . It is also suggested by some features of the RHIC data [8].

Turning to loops in higher representations, we find that the expectation values of *all* renormalized loops are very small in the confined phase. Renormalized loops are nonzero above T_d , with an ordering of expectation values as triplet, octet, and then sextet loop. Even though the octet and sextet condensates are smaller than that for the triplet, they are still significant.

The apparently large values for the condensates of the octet and sextet loops are illusory. This is because when the fundamental loop condenses, that alone induces expectation values for all higher loops. It is to these induced values that we must compare.

This is clear in the limit of an infinite number of colors [10]. Migdal and Makeenko observed that in $SU(N)$ gauge theories, expectation values factorize at large N [40, 41, 42, 43, 44, 45, 46, 47, 48, 49, 50, 51, 52]. Factorization is the statement that disconnected diagrams, with the most traces, dominate at large N .

At infinite N , factorization fixes the expectation value of any Polyakov loop to be equal to powers of those for the fundamental and anti-fundamental, $\tilde{\ell}_{\overline{N}} = (\tilde{\ell}_N)^*$, loop [41]:

$$\langle \tilde{\ell}_{\mathcal{R}} \rangle = \langle \tilde{\ell}_N \rangle^{p_+} \langle \tilde{\ell}_{\overline{N}} \rangle^{p_-} + O\left(\frac{1}{N}\right) . \quad (6)$$

Hence

$$\langle \tilde{\ell}_{\mathcal{R}} \rangle = e^{ie\kappa\phi} \left| \langle \tilde{\ell}_N \rangle \right|^p + O\left(\frac{1}{N}\right) . \quad (7)$$

The integers p_+ and p_- are determined from the Young tableaux of the representation \mathcal{R} , using the composite

representations of Gross and Taylor [52, 53]. At any N , the overall phase is fixed, trivially, by the $Z(N)$ charge of \mathcal{R} , $e_{\mathcal{R}} \equiv p_+ - p_-$, modulo N . What is not trivial is the magnitude of the loop: at large N , the term with the most powers of the fundamental loop dominates, with power $p \equiv p_+ + p_-$.

Lattice simulations with two colors by Damgaard and others [54, 56] showed that the bare adjoint loop is an approximate order parameter for deconfinement. At infinite N , by factorization any renormalized loop serves as an order parameter for deconfinement, independent of its $Z(N)$ charge. For example, consider the adjoint loop, with $p_+ = p_- = 1$, and the loop for the symmetric two-index tensor representation, $p_+ = 2$ and $p_- = 0$. While the adjoint has no $Z(N)$ charge, and the two-index tensor charge two, modulo N , in magnitude both expectation values are $\sim |\langle \tilde{\ell}_N \rangle|^2$ at large N .

We tested these large N relationships numerically for three colors. For each loop, we define the difference between the measured loop and its value in the large N limit. The expectation value of the sextet difference is defined to be

$$\langle \delta \tilde{\ell}_6 \rangle = \langle \tilde{\ell}_6 \rangle - \langle \tilde{\ell}_3 \rangle^2, \quad (8)$$

and that for the octet difference as

$$\langle \delta \tilde{\ell}_8 \rangle = \langle \tilde{\ell}_8 \rangle - |\langle \tilde{\ell}_3 \rangle|^2. \quad (9)$$

Of course there is some ambiguity in defining the difference loops. One advantage of the above definitions is that they automatically vanish at both low and high temperature. In the confined phase, $T \leq T_d$, the difference loops (nearly) vanish because all loops are (essentially) zero; at very high temperature, the difference loops vanish because all loops approach one as $T \rightarrow \infty$.

The expectation values of the difference loops show interesting behavior. They vanish below T_d , and spike down above T_d , with a maximum at a temperature $> T_d$. The spike for the octet difference is smaller, narrower, and closer to T_d than the spike for the sextet difference: $|\langle \delta \tilde{\ell}_8 \rangle| \leq .2$, with a maximum at $\approx 1.1T_d$, while $|\langle \delta \tilde{\ell}_6 \rangle| \leq .25$, with a maximum at $\approx 1.3T_d$.

The magnitude of these expectation values are in accord with a large N expansion. Corrections to the sextet difference are larger, $\delta \tilde{\ell}_6 \sim 1/N$, than those for the octet difference, $\delta \tilde{\ell}_8 \sim 1/N^2$. Thus our measurements of the values of renormalized loops give us a numerical estimate of just how good a large N approximation is for three colors. Corrections to the sextet difference, of $\sim 1/N$, are found to be $\leq 25\%$ when $N = 3$.

Although factorization tells us how to reduce condensates for higher loops to powers of that for the fundamental loop, it does not tell us how the condensate for the fundamental loop changes with temperature. Given the mean field relations satisfied by loops in higher representations, in sec. IV we consider a mean field theory for the fundamental loop itself. We

consider a matrix valued mean field theory, or matrix model; this arises in a wide variety of contexts [41, 42, 43, 44, 45, 46, 47, 48, 49, 50, 51, 52], including previous [48, 49, 54] and recent [14, 15, 16] work on the deconfining transition.

The most general effective action for a matrix model of the deconfining transition involves a sum over loops in all representations. For three colors, we find that the lattice data for the renormalized triplet loop is approximately described by a model whose action includes only the triplet loop. Over the range of temperatures studied, the coupling constant for the triplet loop is nearly linear in temperature. While the overall values of the sextet and octet loops are approximately described by this mean field theory, the difference loops are not. We categorize more involved models which might.

It is interesting to consider what matrix models might apply to the deconfining transition for more than three colors. Consider the simplest possible model, where the action includes just the fundamental loop. At infinite N , the solution follows from that of Gross and Witten [14, 15, 16, 43, 47, 49, 51, 54]. Kogut, Snow, and Stone showed that in this model, the deconfining transition is of first order, with a latent heat $\sim N^2$ [14, 15, 47, 49, 51, 54]. As a first order transition, the fundamental loop jumps, from zero to precisely one half:

$$|\langle \tilde{\ell}_N \rangle| = \frac{1}{2}, \quad T = T_d^+, \quad N = \infty. \quad (10)$$

This was also stressed recently by Aharony, Marsano, Minwalla, Papadodimas, and Van Raamsdonk [14]: at T_d , this theory only deconfines *halfway*.

It is striking that this special value at large N is close to that found from numerical simulations for the renormalized, triplet loop; both we and Kaczmarek *et al.* [39] find $|\langle \tilde{\ell}_3 \rangle| \approx .4$ at $T = T_d^+$. In the $N = 3$ matrix model closest to the Gross–Witten point, this value is not $\frac{1}{2}$, but $\approx .485 \pm .001$ [47, 54, 55]. The value in the Polyakov loop model, which we discuss shortly, is $\approx .55$ [19].

The first order transition at the Gross–Witten point is atypical. In ordinary first order transitions, masses are nonzero on either side of the transition [38]. Even though the value of the fundamental loop jumps at T_d , at the Gross–Witten point both the string tension, and a gauge invariant Debye mass, vanish. This is only possible because of a transition, which is of third order in the matrix model coupling constant, at infinite N [43]. The Gross–Witten point is specific to infinite N : at finite N , but ≥ 3 , in the matrix model deconfinement is an ordinary first order transition, with the string tension and the Debye mass nonzero at T_d .

For three colors, lattice simulations find a relatively weak first order transition, accompanied by a large decrease in both the string tension and the Debye mass near T_d , each by about a factor of ten [25]. The customary explanation for this is that, as in the Potts model, three colors is near the second order transition known to occur for two colors [56]. We suggest that the deconfi-

ing phase transition for three colors is also close to the Gross–Witten point of infinite N ; exactly how close can be categorized in a matrix model [55].

Aharony *et al.* [14] showed how at large N the Hagedorn temperature can be computed when space is a very small sphere. They find that the deconfining transition is of first order if the Hagedorn temperature is greater than T_d . It is tempting to think that the spikes which we found for the sextet and octet difference loops may be related to the Hagedorn temperature. If so, for three colors the Hagedorn temperature is tens of percent above that for the deconfining transition.

It would be valuable to know from numerical simulations if the deconfining transition for more than three colors is close to the Gross–Witten point as well, or if that is unique to three colors.

An Appendix gives a formal discussion of improved Wilson lines; on the lattice, these are related to smeared, stout links [57]. This may be of use for measuring Polyakov loops in higher representations.

Our work was motivated by the Polyakov loop model, which postulates a relationship between the Polyakov loop — which was presumed to exist as a renormalized quantity — and the pressure [18, 19, 20, 21]. In the end, we have more than expected: not just a renormalized Polyakov loop, but a good approximation to its potential, in the $SU(3)$ matrix model.

II. BARE AND RENORMALIZED POLYAKOV LOOPS

A. Traces of Wilson lines in imaginary time

At a temperature T , the thermal Wilson line at a spatial point \vec{x} , running in time from 0 to τ , is

$$\mathbf{L}_{\mathcal{R}}(\vec{x}, \tau) = \mathcal{P} \exp \left(ig \int_0^\tau A_0^a(\vec{x}, \tau') \mathbf{t}_{\mathcal{R}}^a d\tau' \right) ; \quad (11)$$

we take the representation \mathcal{R} to be irreducible. The notation is standard: \mathcal{P} denotes path ordering, g is the gauge coupling constant, τ and τ' are variables for imaginary time, $\tau, \tau' : 0 \rightarrow 1/T$, A_0^a is the vector potential in the time direction, and $\mathbf{t}_{\mathcal{R}}^a$ are the generators of $SU(N)$ in \mathcal{R} .

The Wilson line is a $SU(N)$ phase factor for \mathcal{R} , and so is a unitary matrix,

$$\mathbf{L}_{\mathcal{R}}^\dagger(\vec{x}, \tau) \mathbf{L}_{\mathcal{R}}(\vec{x}, \tau) = \mathbf{1}_{d_{\mathcal{R}}} ; \quad (12)$$

$d_{\mathcal{R}}$ is the dimension of the representation, and $\mathbf{1}_{d_{\mathcal{R}}}$ the unit matrix in that space.

The thermal Wilson line is proportional to the propagator of a “test” quark in the representation \mathcal{R} [21, 33]. A test quark is one whose mass is so large that if you put it at a given point in space, \vec{x} , it just sits there. The only motion of a test quark is up in imaginary time. While the test quark doesn’t move in space, it still interacts in color

space: through the Aharonov–Bohm effect, it acquires a $SU(N)$ phase.

To see this, form a covariant derivative in imaginary time, and define a propagator, $\mathcal{G}_{\mathcal{R}}$, as its inverse:

$$\left(\frac{d}{d\tau} \mathbf{1}_{d_{\mathcal{R}}} - ig A_0^a(\vec{x}, \tau) \mathbf{t}_{\mathcal{R}}^a \right) \mathcal{G}_{\mathcal{R}}(\vec{x}, \tau) = \delta(\tau) \mathbf{1}_{d_{\mathcal{R}}} . \quad (13)$$

It is easy computing the propagator in one dimension: it is just a step function, $\theta(\tau)$, times the Wilson line,

$$\mathcal{G}_{\mathcal{R}}(\vec{x}, \tau) = \theta(\tau) \mathbf{L}_{\mathcal{R}}(\vec{x}, \tau) . \quad (14)$$

Alternately, consider the path integral representation for the propagator of a particle with mass m in a background gauge field; schematically,

$$\int \mathcal{D}x^\mu \exp \left(- \int \left(m\sqrt{\dot{x}^2} + ig A_\mu \dot{x}^\mu \right) ds \right) , \quad (15)$$

where $\dot{x}^\mu = dx^\mu/ds$, and s is the path length; an exact form is given in [31]. In the limit of $m \rightarrow \infty$, this path is a straight line up in imaginary time, and this propagator is the thermal Wilson line. Classically, the partition function in (15) is $\sim \exp(-m\mathcal{L})$, where m is the bare mass, and \mathcal{L} is the length of the path.

Under a gauge transformation in \mathcal{R} , $\Omega_{\mathcal{R}}(\vec{x}, \tau)$, the Wilson line transforms as

$$\mathbf{L}_{\mathcal{R}}(\vec{x}, \tau) \rightarrow \Omega_{\mathcal{R}}^\dagger(\vec{x}, \tau) \mathbf{L}_{\mathcal{R}}(\vec{x}, \tau) \Omega_{\mathcal{R}}(\vec{x}, 0) . \quad (16)$$

As bosons, the gauge fields are periodic in imaginary time, with period $1/T$. For the time being, we also assume that all gauge transformations are periodic in time, $\Omega_{\mathcal{R}}(\vec{x}, 1/T) = \Omega_{\mathcal{R}}(\vec{x}, 0)$. We relax that assumption later, but only in a way which affects the global symmetry, and not the local symmetry.

For periodic gauge transformations, we can form a quantity which is locally gauge invariant by wrapping the Wilson line around in imaginary time, and then taking its trace:

$$\text{tr} \mathbf{L}_{\mathcal{R}}(\vec{x}, 1/T) . \quad (17)$$

For the time being we follow the custom of mathematics, which is to work with traces which are not normalized. The trace is greatest when the Wilson line is the identity, $= d_{\mathcal{R}}$.

The propagation of a test quark, at \vec{x} , forward in imaginary time generates the Wilson line in the fundamental representation, $\mathbf{L}_N(\vec{x}, 1/T)$. A test anti-quark is a test quark moving backward in imaginary time, so it gives the conjugate Wilson line, $\mathbf{L}_{\overline{N}}(\vec{x}, 1/T) = \mathbf{L}_N^\dagger(\vec{x}, 1/T)$.

Let us consider how to combine more test quarks and anti-quarks. To be gauge invariant, the Wilson lines must wrap around completely in imaginary time, so we drop the dependence on imaginary time, $1/T$. We also assume that all test quarks and anti-quarks are put down at the same point in space, and so drop the dependence on \vec{x}

as well. So a test quark gives \mathbf{L}_N , and a test anti-quark, \mathbf{L}_N^\dagger .

The general classification of representations is, for arbitrary N , rather involved [52, 53]. We thus start with the lowest representations for general N . We then discuss some simplifications for $N = 3$. Finally, we show how one can easily classify all representations in the large N limit [52]. We use a notation where \mathcal{R} is generally denoted by its dimension, $d_{\mathcal{R}}$.

1. Simple examples

The adjoint Wilson line is a test meson, constructed from a test quark and anti-quark. To combine the fundamental and anti-fundamental Wilson lines into something with adjoint indices, we sandwich \mathbf{L}_N and \mathbf{L}_N^\dagger between two $SU(N)$ generators, t_N^a ,

$$\mathbf{L}_{N^2-1}^{ab} = \text{tr} \left(\mathbf{L}_N t_N^a \mathbf{L}_N^\dagger t_N^b \right); \quad (18)$$

the adjoint indices $a, b = 1 \dots (N^2 - 1)$. The trace of the adjoint Wilson line is

$$\text{tr} \mathbf{L}_{N^2-1} = |\text{tr} \mathbf{L}_N|^2 - 1. \quad (19)$$

This follows from an identity on the t^a 's, or directly from group theory. The product of the fundamental and anti-fundamental representations is the sum of the adjoint and identity, so the coefficient of $|\text{tr} \mathbf{L}_N|^2$ in (19) is one. To check the -1 in (19), consider the case when the Wilson line is the unit matrix, $\mathbf{L}_N = \mathbf{1}_N$; then the adjoint trace is its dimension, $= N^2 - 1$.

The next representations are tensors with two fundamental indices [53]. These represent the propagation of two test quarks up in imaginary time. Two Wilson lines can be put together in either a symmetric (+), or an anti-symmetric (-), way. The Wilson lines for the two-index representations are

$$\mathbf{L}_{(N^2 \pm N)/2}^{ij;kl} = \frac{1}{2} \left(\mathbf{L}_N^{ik} \mathbf{L}_N^{jl} \pm \mathbf{L}_N^{jk} \mathbf{L}_N^{il} \right). \quad (20)$$

Here $i, j, k, l = 1 \dots N$ are indices for the fundamental representation. The traces of the representations with two Wilson lines are then

$$\text{tr} \mathbf{L}_{(N^2 \pm N)/2} = \frac{1}{2} \left((\text{tr} \mathbf{L}_N)^2 \pm \text{tr} \mathbf{L}_N^2 \right). \quad (21)$$

Checking the coefficients for $\mathbf{L}_N = \mathbf{1}_N$, the dimensions of the representations are as indicated. The first term is a product of two Wilson lines, each of which wrap around once in imaginary time. The second term is one Wilson line which wraps around twice in imaginary time.

2. Three colors

For three colors, the fundamental representation is a triplet, $\mathbf{3}$, the adjoint representation is an octet, $\mathbf{8}$, and the symmetric two-index representation is a sextet, $\mathbf{6}$.

Special to three colors, the anti-symmetric two-index representation is the anti-triplet, $\bar{\mathbf{3}}$. To see this, diagonalize the triplet Wilson line by a local gauge rotation. After diagonalization, each element of \mathbf{L}_3 is a phase; the product of all phases is one:

$$\mathbf{L}_3 = \begin{pmatrix} \exp(i\alpha_1) & 0 & 0 \\ 0 & \exp(i\alpha_2) & 0 \\ 0 & 0 & \exp(-i(\alpha_1 + \alpha_2)) \end{pmatrix}. \quad (22)$$

Then it is easy to check that $\mathbf{L}_{(N^2-N)/2}$ from (21) $= \text{tr} \mathbf{L}_3^\dagger$ when $N = 3$. Notice that (21) actually gives the anti-triplet loop, which is a fault of our notation.

We mention one other representation for three colors. Consider a test baryon, composed of three test quarks. The symmetric combination of three fundamental Wilson lines gives the decuplet representation when $N = 3$. Its trace is

$$\text{tr} \mathbf{L}_{10} = \frac{1}{6} \left((\text{tr} \mathbf{L}_3)^3 + 3 \text{tr} \mathbf{L}_3 \text{tr} \mathbf{L}_3^2 + 2 \text{tr} \mathbf{L}_3^3 \right). \quad (23)$$

Since \mathbf{L}_3 is a $SU(3)$ matrix,

$$\det \mathbf{L}_3 = 1$$

$$= \frac{1}{6} \left((\text{tr} \mathbf{L}_3)^3 - \frac{1}{2} \text{tr} \mathbf{L}_3 \text{tr} \mathbf{L}_3^2 + \frac{1}{3} \text{tr} \mathbf{L}_3^3 \right), \quad (24)$$

which is Mandelstam's constraint [59]. Using it, we find that the trace of the decuplet Wilson line is

$$\text{tr} \mathbf{L}_{10} = \text{tr} \mathbf{L}_3 \text{tr} \mathbf{L}_3^2 + 1. \quad (25)$$

3. Large N

The usual classification of representations is given using Young tableaux [52, 53]. This is not very convenient for the large N limit, though. The reason is elementary: Young tableaux involve the construction of tensors with fundamental indices. While of course complete, it does not naturally incorporate the symmetry between the fundamental and anti-fundamental representations. This is accomplished using the composite representations of Gross and Taylor [52]; we give an abbreviated summary which is sufficient for our purposes.

Consider forming a state with p_+ test quarks and p_- test anti-quarks. This is done by combining p_+ fundamental Wilson lines, and p_- anti-fundamental Wilson lines, in all possible ways. To be gauge invariant, we must take traces of \mathbf{L}_N and \mathbf{L}_N^\dagger . We also have to remember that \mathbf{L}_N is a unitary matrix, $\mathbf{L}_N^\dagger \mathbf{L}_N = \mathbf{1}_N$, (12). This relation implies that all traces are either traces of powers of \mathbf{L}_N , or traces of powers of \mathbf{L}_N^\dagger , separately. Any mixed terms can be simplified using the unitary relation.

The explicit construction of Wilson lines in different representations, as done above for the adjoint and the

two-index tensor, is unnecessary. Only gauge invariant quantities matter: these are traces of the Wilson line in different representations. For any \mathcal{R} , by the Frobenius formula [52, 53] we can express the trace of a Wilson line in \mathcal{R} as sums of products of traces of the fundamental Wilson line.

We do this naively, by considering how to combine p_+ \mathbf{L}_N 's and p_- \mathbf{L}_N^\dagger 's. The simplest thing is to take a trace of every Wilson line, separately:

$$(\text{tr } \mathbf{L}_N)^{p_+} (\text{tr } \mathbf{L}_N^\dagger)^{p_-} . \quad (26)$$

In this term, each Wilson line wraps once, and only once, around in imaginary time.

This is just the first term in a long series, though. To start with, we can consider a term where one Wilson line wraps around twice in imaginary time:

$$(\text{tr } \mathbf{L}_N)^{p_+-2} (\text{tr } \mathbf{L}_N^2) (\text{tr } \mathbf{L}_N^\dagger)^{p_-} . \quad (27)$$

Continuing, a term where one Wilson line wraps around thrice:

$$(\text{tr } \mathbf{L}_N)^{p_+-3} (\text{tr } \mathbf{L}_N^3) (\text{tr } \mathbf{L}_N^\dagger)^{p_-} , \quad (28)$$

and so on. We can do this as well for the anti-Wilson lines; a Wilson line which wraps around backward twice gives

$$(\text{tr } \mathbf{L}_N)^{p_+} (\text{tr } \mathbf{L}_N^\dagger)^{p_- - 2} \text{tr } (\mathbf{L}_N^\dagger)^2 . \quad (29)$$

We continue in this fashion. The series continues down, generating fewer traces overall, as they are replaced by traces with higher powers of the Wilson and anti-Wilson line. In general, the operator $\text{tr } \mathbf{L}^{p_+}$ represents a Wilson line which wraps around p_+ times forward in imaginary time; $\text{tr } (\mathbf{L}^\dagger)^{p_-}$, a Wilson line which wraps around p_- times backward.

The series stops when we only have either one or no traces left. If $p_+ = p_-$, the series stops at a constant, with no trace. If $p_+ \neq p_-$, the series stops at one trace,

$$\text{tr } \mathbf{L}_N^{p_+} (\mathbf{L}_N^\dagger)^{p_-} . \quad (30)$$

This term can obviously be reduced, as it is a Wilson line which goes forward p_+ times, and then backward p_- times.

The above series of traces of Wilson lines represents the propagation of test quarks and anti-quarks. All we can do with test quarks is to take loops in imaginary time, so the only question left is how many times a test quark, or anti-quark, goes around in imaginary time.

When $p_- = 0$ these terms are the Schur functions [52, 53]. When $p_- \neq 0$, these terms are the Schur functions for the composite representations of [52].

Consider now the powers of N at large N . We assume that in the deconfined phase, each trace gives a power of N : $\text{tr } \mathbf{L}_N^q \sim N$ for all q . The first term in (26) is of order $\sim N^p$. Terms in (27) and (29) have one fewer trace overall, and so are $\sim N^{p-1}$, down by one power of $1/N$

relative to (26). Each time a Wilson line wraps around an extra time in imaginary time, a possible trace is lost, which suppresses the term by $\sim 1/N$ relative to (26).

This assumes that the coefficients of all terms, (26-30), are of order one. For example, if the coefficient of (27) or (29) were $\sim N$ relative to that of (26), then we couldn't conclude anything about the large N limit. Group theory tells us, however, that this is not so: for any N , all coefficients are numbers of order one [52, 53]. This is because all representations are constructed by symmetrization and anti-symmetrization operators [53]; the action of these operators depends on the number of indices, but not upon N .

Consequently, at large N the trace of any representation is dominated by the term where every Wilson line (or anti-line) wraps around only once in imaginary time. This is just because we maximize the number of possible traces, and so the powers of N . At large N we denote representations as $\mathcal{R} = N \wedge p$:

$$\text{tr } \mathbf{L}_{N \wedge p} \sim (\text{tr } \mathbf{L}_N)^{p_+} (\text{tr } \mathbf{L}_N^\dagger)^{p_-} , \quad (31)$$

$p = p_+ + p_-$. The notation is meant to be suggestive, as the dimension of this representation is $\sim N^p$ at large N .

The integers p_+ and p_- can be computed from the Young tableaux of the representation [52]. Denote the columns of the Young tableaux by the index i , and separate them into two categories. If the number of rows in a column, r^i , is $\leq N/2$, then we leave the column alone, and refer to it as a fundamental column, with $r_+^i = r^i$ rows. If the number of rows in a column is $> N/2$, then we turn it into a column with $r_-^i = N - r^i$ anti-fundamental rows. Then $p_+ = \sum_i r_+^i$ is the number of boxes in all of the fundamental columns, and $p_- = \sum_i r_-^i$ is the number of boxes in all of the anti-fundamental columns. In the limit of infinite N , no other details of the Young tableaux matter; all that matters is the total number of boxes p_+ and p_- .

In group theory, the distinction between fundamental and anti-fundamental columns appears awkward. It is essential to understand the large N limit, though. Consider, for example, a single anti-fundamental box in a Young tableaux: this is given by a column with $N - 1$ rows. If we counted rows naively, this would give us $N - 1$ powers of a trace. Clearly we should replace this by one anti-fundamental line, and one trace. Geometrically, if a Wilson line wraps forward around r_i times in imaginary time, when $r_i > N/2$ it is better to replace it by a Wilson line going backward $N - r_i$ times.

While we do not need it now, we note that the Casimirs of the representations $\mathbf{N} \wedge \mathbf{p}$ were computed by Samuel [46] and Gross and Taylor [52]. While the dimension grows strongly, like N^p , the Casimir does not; at large N , it is linear in N , proportional to $p_+ + p_-$:

$$\mathcal{C}_{\mathbf{N} \wedge \mathbf{p}} = (p_+ + p_-) \frac{N}{2} + O(1) . \quad (32)$$

We shall see in sec (II.D) that this relation for the Casimir ensures that Polyakov loops, as computed to lowest order

in perturbation theory, satisfy factorization at large N , (58) and (55).

B. $Z(N)$ charges and confinement

Previously, we required that gauge transformations be strictly periodic in imaginary time. 't Hooft noted that this is not necessary. Consider gauge transformations which are periodic, in $1/T$, only up to a constant. So as not to change the periodicity of the gauge fields, this constant gauge transformation must be equal to the identity matrix times a phase, equal to an N^{th} root of unity, (2). For the fundamental representation, aperiodic gauge transformations are

$$\Omega_N(\vec{x}, 1/T) = e^{i\phi} \Omega_N(\vec{x}, 0) \quad , \quad e^{i\phi N} = 1 \quad . \quad (33)$$

This phase represents the center of the local $SU(N)$ gauge group, which is a global group of $Z(N)$: $\phi = 2\pi j/N$, $j = 0, 1 \dots (N-1)$.

As the $Z(N)$ phases commute with any element of the group, the gauge fields remain strictly periodic under such an aperiodic gauge transformation. The Wilson line, however, does change: for the fundamental representation,

$$\mathbf{L}_N \rightarrow e^{i\phi} \mathbf{L}_N \quad . \quad (34)$$

We define the $Z(N)$ charge, or the N -ality, of the fundamental Wilson line to be one, $e_N = 1$. The traces of Wilson lines in other representations transform under aperiodic gauge transformations as

$$\mathbf{L}_{\mathcal{R}} \rightarrow e^{ie_{\mathcal{R}}\phi} \mathbf{L}_{\mathcal{R}} \quad ; \quad (35)$$

the $Z(N)$ charge $e_{\mathcal{R}}$ is an integer.

Due to the cyclic nature of $Z(N)$, charge is only defined modulo N . If the fundamental has charge one, the anti-fundamental has charge minus one, which is equivalent to charge $N-1$. The simplest field with vanishing $Z(N)$ charge is the adjoint. A baryon Wilson line, such as the symmetric combination of N fundamental indices, is also $Z(N)$ neutral. At large N , the Wilson line in the $\mathbf{N} \wedge \mathbf{p}$ representation of (31) has $Z(N)$ charge $e_{\mathcal{R}} = p_+ - p_-$, modulo N .

For three colors, the anti-triplet and sextet representations have charge two, which is the same as minus one. As a test baryon, the decuplet Wilson line is $Z(3)$ neutral.

The confining phase, for $T \leq T_d$, is characterized by an unbroken global $Z(N)$ symmetry [1]. Hence the traces of Wilson lines with nonzero $Z(N)$ charge vanish below T_d ,

$$\langle \text{tr } \mathbf{L}_{\mathcal{R}} \rangle = 0 \quad , \quad T < T_d \quad , \quad e_{\mathcal{R}} \neq 0 \quad . \quad (36)$$

Above T_d , all traces develop expectation values,

$$\langle \text{tr } \mathbf{L}_{\mathcal{R}} \rangle \neq 0 \quad , \quad T > T_d \quad , \quad \forall e_{\mathcal{R}} \quad . \quad (37)$$

(Implicitly, we always assume that symmetry breaking occurs when a background $Z(N)$ field is applied, and then allowed to vanish, in the appropriate infinite volume limit.)

A priori, it is not obvious how the traces of $Z(N)$ neutral Wilson lines behave in the confined phase, $T < T_d$. Certainly, they must be nonzero at *all* temperatures. Even for $T < T_d$, they are not protected by the $Z(N)$ symmetry, and so are induced by quantum fluctuations at some level. For three colors, though, numerically we find that the expectation value of the renormalized octet loop is very small below T_d , (63). This is natural in a matrix model, as discussed at the end of Sec. (IV.C).

There is a counterpart to this in the behavior of large adjoint Wilson loops. At zero temperature, a fundamental Wilson loop forms a string, with its expectation value the exponential of the string tension times the area. Adjoint Wilson loops screen, so the adjoint string tension vanishes. Greensite and Halpern [40] show that at large N , the adjoint string breaks over distances which grow as $\sim \log(N)$. Similarly, the lattice finds that the adjoint string only breaks over large distances [29].

C. From traces of Wilson lines to Polyakov loops

Traces of Wilson lines grow with the dimensionality of the representation. It is convenient to introduce a normalized quantity, which approaches one in the obvious perturbative limit. From the expectation value of the Wilson line in a given representation, we define the expectation value of the Polyakov loop, $\ell_{\mathcal{R}}$, as

$$\langle \ell_{\mathcal{R}} \rangle = \frac{1}{d_{\mathcal{R}}} \langle \text{tr } \mathbf{L}_{\mathcal{R}} \rangle \quad . \quad (38)$$

The phase of the expectation of a given loop is fixed by the $Z(N)$ symmetry. In the perturbative limit at high temperature, $\mathbf{L}_{\mathcal{R}} \rightarrow e^{ie_{\mathcal{R}}\phi} \mathbf{1}_{\mathcal{R}}$, and $\ell_{\mathcal{R}} \rightarrow e^{ie_{\mathcal{R}}\phi}$.

Using normalized loops, instead of just traces, is most useful in considering the limit of a large number of colors. For example, the adjoint loop is

$$\ell_{N^2-1} = \frac{1}{N^2-1} \text{tr } \mathbf{L}_{N^2-1} = \frac{N^2}{N^2-1} \left(|\ell_N|^2 - \frac{1}{N^2} \right) \quad . \quad (39)$$

The large N limit of this expression cannot be taken directly, since it involves an operator, $|\ell_N|^2$, and a pure number. A large N limit can be taken by comparing expectation values. This is especially easy at large N , as then disconnected diagrams dominate, and all expectation values factorize [40, 41, 42, 43, 44, 45, 46, 47, 48, 49, 50, 51, 52]. For instance,

$$\langle |\ell_N|^2 \rangle = \langle \ell_N \rangle^2 \quad , \quad N = \infty \quad . \quad (40)$$

Using this, at large N the expectation value of the adjoint loop is, in magnitude, identically the square of that for

the fundamental loop,

$$\langle \ell_{N^2-1} \rangle \approx |\langle \ell_N \rangle|^2 + O\left(\frac{1}{N^2}\right). \quad (41)$$

As it stands, this is a relationship between bare loops; we shall see, however, that it survives renormalization.

For the two index tensor representations,

$$\begin{aligned} \ell_{(N^2 \pm N)/2} &= \frac{2}{N(N \pm 1)} \text{tr } \mathbf{L}_{(N^2 \pm N)/2} \\ &= \frac{N}{N \pm 1} \left(\ell_N^2 \pm \frac{1}{N^2} \text{tr } \mathbf{L}_N^2 \right) \end{aligned} \quad (42)$$

Hence at $N = \infty$ the expectation values of the two-index tensor loops are the square of the fundamental loop,

$$\langle \ell_{(N^2 \pm N)/2} \rangle \approx \langle \ell_N \rangle^2 + O\left(\frac{1}{N}\right). \quad (43)$$

Notice that the term at infinite N is the same for both the symmetric and the anti-symmetric representation; the difference only shows up in corrections in $1/N$. This generalizes to higher representations at large N .

For the two index tensor representations, corrections in $1/N$ start with the expectation value of the operator

$$\frac{1}{N} \left(\frac{1}{N} \text{tr } \mathbf{L}_N^2 \right). \quad (44)$$

In the deconfined phase, we consider the trace of any power of the Wilson line to be a number of order one, so the trace of \mathbf{L}_N^2 is like that of \mathbf{L}_N , a number of order N . Overall, then, this operator is $\sim 1/N$. It is not surprising that corrections to the two-index loop are $\sim 1/N$, larger than the $\sim 1/N^2$ for the corrections to the adjoint loop. These corrections for the two-index loop arise because the operator has $Z(N)$ charge two, and so mix with the operator in (44). The adjoint loop is $Z(N)$ neutral, and so can't mix with this operator. The analogous operator for the adjoint loop is $\text{tr } \mathbf{L}_N^\dagger \mathbf{L}_N$, which by the unitary relation of (12) is a constant.

The generalization to the $\mathbf{N} \wedge \mathbf{p}$ representations of the large N limit is immediate,

$$\langle \ell_{\mathbf{N} \wedge \mathbf{p}} \rangle = \langle \ell_N \rangle^{p+} \langle \ell_N^* \rangle^{p-} + O\left(\frac{1}{N}\right), \quad (45)$$

which is (6) and (7). One advantage of using loops is that it is easy to check overall normalization: up to $Z(N)$ phases, both sides approach unity in the perturbative limit.

A systematic expansion in $1/N$ proceeds by including operators such as

$$\frac{1}{N^{q-1}} \left(\frac{1}{N} \text{tr } \mathbf{L}_N^q \right), \quad (46)$$

for integral q . This operator is $\sim 1/N^{q-1}$ in the deconfined phase. As q grows, the number of such operators does as well. We do not concern ourselves here with the development of a systematic expansion, and consider only the leading corrections in $1/N$. For three colors, our numerical simulations indicate that this might not be such a bad approximation.

Even to leading order at large N , some representations involve loops other than the fundamental. Consider a test baryon, composed of N fundamentals. Because of Mandelstam's constraint that \mathbf{L}_N is an $SU(N)$ matrix, $\det \mathbf{L}_N = 1$, the term with N powers of the fundamental loop is part of the identity representation. Hence at large N , the loop for a test baryon behaves as

$$\langle \ell_{\text{test-baryon}} \rangle = \langle \ell_N \rangle^{N-1} \left\langle \frac{1}{N} \text{tr } \mathbf{L}_N^2 \right\rangle + O\left(\frac{1}{N}\right). \quad (47)$$

This is illustrated by the decuplet loop for three colors, (25).

D. Renormalization of Polyakov loops

With this lengthy introduction aside, we turn to the problem at hand, the renormalization of Polyakov loops.

Remember how mass renormalization usually works, as for a scalar field, ϕ , in four spacetime dimensions [38]. If the mass of the field is m , and its coupling $\lambda \phi^4$, to one loop order the mass squared receives contributions

$$\sim \lambda \int^\Lambda \frac{d^4 k}{k^2 + m^2} \sim \lambda \Lambda^2, \quad \lambda m^2 \log\left(\frac{\Lambda}{m}\right); \quad (48)$$

a momentum cutoff Λ is used to regularize the integral. The structure at one loop order is generic to perturbation theory: there are two mass divergences, one proportional to a power of the cutoff, $\sim \Lambda^2$, and the other, to a logarithm of the cutoff, $\sim m^2 \log(\Lambda/m)$. The power divergence is an additive shift in the bare mass, and for a scalar field is inconsequential: the parameters are tuned to be near a critical point, where the renormalized mass vanishes. On the other hand, the logarithmic divergence is physical, related to the anomalous dimension for the mass operator. A renormalization condition is required to fix the value of the renormalized mass at a given scale.

Polyakov loops correspond to a test particle whose mass is taken to infinity, so their worldline is a straight line. This freezes out fluctuations in the time-like direction. This is obvious in perturbation theory: as $\int A_0(\vec{x}, \tau) d\tau$ always enters, only modes which are constant in τ appear. Thus the mass divergence of a Polyakov loop in four spacetime dimensions is like that of a propagating particle in one less dimension, which is three. Similarly, the mass divergences of a scalar field in four spacetime dimensions, (48), are like those of Polyakov loops in five spacetime dimensions.

The ultraviolet divergences of a Wilson line depend only upon the representation, and not upon (smooth)

details of the path. For the time being, let $\mathbf{L}_{\mathcal{R}}$ denote any Wilson line in a representation \mathcal{R} ; we only assume that the path forms a loop, so that traces of $\mathbf{L}_{\mathcal{R}}$ are gauge invariant. The expectation value of the Wilson line has a mass divergence which depends upon the length of the loop, \mathcal{L} , as

$$\langle \text{tr } \mathbf{L}_{\mathcal{R}} \rangle \sim \exp(-m_{\mathcal{R}}^{\text{div}} \mathcal{L}) . \quad (49)$$

The exponentiation of mass divergences follows from the analysis of Gervais and Neveu [31]. Similar to (15), they rewrite the Wilson line as a propagator for a fermion which lives in one dimension, along the path of the loop. With lattice regularization, the additive mass shift which the Wilson loop undergoes, $m_{\mathcal{R}}^{\text{div}}$, is no different from that which (non-gauged) propagating fields also experience, such as for massive quarks, or scalar fields, ϕ .

On the lattice, the exponentiation of mass divergences has been shown explicitly by Curci, Menotti, and Paffuti to $\sim g^4$ [37].

To develop insight into the divergent masses, we compute to one loop order. In four spacetime dimensions,

$$m_{\mathcal{R}}^{\text{div}} \sim + \mathcal{C}_{\mathcal{R}} g^2 \int^{1/a} \frac{d^3 k}{k^2} \sim + \frac{\mathcal{C}_{\mathcal{R}} g^2}{a} . \quad (50)$$

We have used a lattice, with lattice spacing a , to regularize the theory. The exact coefficient of $1/a$ in $m_{\mathcal{R}}^{\text{div}}$ depends on the details of the lattice discretization, but it is a positive, nonzero number of order one. In four dimensions, $a m_{\mathcal{R}}^{\text{div}}$ is a power series in the coupling constant.

For a straight Polyakov loop in four dimensions, this is the only divergence: there is no anomalous dimension for the corresponding mass. This is clear to any order in perturbation theory, and occurs because the mass divergence is like that of a particle which propagates in three, instead of four, dimensions.

Loops can also have cusps [32, 33, 34, 35, 36]. In order to be periodic in imaginary time, the simplest example of a Polyakov loop with cusps has not one, but two, cusps. This is illustrated in Fig. 1, with cusps at $\tau = 0$ and $\tau = 1/(2T)$. These cusps reflect external probes which deflect the test particle at these points. As Polyakov loops, the expectation values of single loops with cusps only have nontrivial expectation values in the deconfined phase.

A cusp generates a logarithmic singularity in four spacetime dimensions [32, 33, 34, 35, 36]. This is not proportional to the length, and so does not contribute to the divergent mass. A condition to fix the value of a renormalized loop with a cusp must be supplied, but this is standard. For example, in QCD loops with cusps are related to the Isgur-Wise function [36].

It is also interesting to consider loops in three, instead of four, spacetime dimensions [58]. The linear divergence of (50) is now logarithmic [31],

$$m_{\mathcal{R}}^{\text{div}} \sim + \mathcal{C}_{\mathcal{R}} g^2 \int^{1/a} \frac{d^2 k}{k^2} \sim + \mathcal{C}_{\mathcal{R}} g^2 \log\left(\frac{1}{a}\right) ; \quad (51)$$

in three dimensions, the coupling constant g^2 has dimensions of mass. As the divergent mass depends logarithmically upon the lattice spacing, a condition to fix the value of the renormalized loop must be supplied [60]. Loops with cusps do not have new ultraviolet divergences in three spacetime dimensions, although they do have power like infrared divergences.

Defining wave function renormalization for a Wilson line of length \mathcal{L} as

$$\mathcal{Z}_{\mathcal{R}} = \exp(-m_{\mathcal{R}}^{\text{div}} \mathcal{L}) , \quad (52)$$

then the renormalized Wilson line is given by

$$\tilde{\mathbf{L}}_{\mathcal{R}} = \frac{1}{\mathcal{Z}_{\mathcal{R}}} \mathbf{L}_{\mathcal{R}} ; \quad (53)$$

as illustrated by the renormalization of Polyakov loops, (4). In the space of all $SU(N)$ invariant tensors, the set of irreducible representations form a complete and orthonormal basis [53]. As this basis is orthonormal, Wilson lines in different representations do not mix. Consequently, in different representations the divergent masses, $m_{\mathcal{R}}^{\text{div}}$, and so the renormalization constants $\mathcal{Z}_{\mathcal{R}}$, are independent quantities.

We discuss in the next section how to extract the divergent masses from lattice simulations using a straight Wilson line. In an Appendix we also discuss how the Wilson line might be modified to alter the mass divergence.

It is illuminating to compute the renormalized loops to one loop order. Then it is easiest using dimensional regularization, as then the divergent mass automatically vanishes. Following Gava and Jengo [3, 21], the leading correction arises after the Debye mass, $m_D^2 = Ng^2 T^2/3$, is included by resummation. To lowest order, the correction to the renormalized loop is

$$\langle \tilde{\ell}_{\mathcal{R}} \rangle - 1 \approx - \mathcal{C}_{\mathcal{R}} g^2 \int \frac{d^{3-\epsilon} k}{k^2 + m_D^2} \sim + \mathcal{C}_{\mathcal{R}} g^2 m_D \quad (54)$$

so that

$$\langle \tilde{\ell}_{\mathcal{R}} \rangle \approx 1 + \frac{\mathcal{C}_{\mathcal{R}} (g^2 N)^{3/2}}{8\pi N \sqrt{3}} + O(g^4) . \quad (55)$$

(In three spacetime dimensions, $\langle \tilde{\ell}_{\mathcal{R}} \rangle - 1 \approx \mathcal{C}_{\mathcal{R}} (g^2/T) \log(T/g^2)$ [60].)

In four spacetime dimensions, the leading correction to the renormalized loop is positive. Thus in the limit of high temperature, the loop approaches one from above, and not from below. At first sight, this seems paradoxical. Bare Polyakov loops are traces of $SU(N)$ matrices, and so satisfy a strict inequality, $|\ell_{\mathcal{R}}| \leq 1$. For example, on the lattice this holds configuration by configuration. Instead, renormalized loops satisfy the renormalized constraint,

$$|\tilde{\ell}_{\mathcal{R}}| \leq \frac{1}{\mathcal{Z}_{\mathcal{R}}} . \quad (56)$$

Numerically, we find that the divergent masses are uniformly positive,

$$a m_{\mathcal{R}}^{div} > 0, \quad (57)$$

for all representations, at all temperatures. If so, then the renormalization constant $\mathcal{Z}_{\mathcal{R}}$ always vanishes in the continuum limit, and there is no constraint on the renormalized loop. This condition is most natural: otherwise, $\mathcal{Z}_{\mathcal{R}}$ diverges as $a \rightarrow 0$, so the renormalized loop must vanish.

The renormalization of a constraint is also familiar from the non-linear sigma model in two spacetime dimensions [38]. If the sigma field is an $SU(N)$ matrix, then like the bare Wilson line, the bare field is a unitary matrix. Because of wave-function renormalization, however, the renormalized sigma field satisfies a renormalized, and not a bare, constraint.

In the large N limit, factorization holds. This implies that

$$a m_{\mathcal{R}}^{div} \approx (p_+ + p_-) a m_N^{div}. \quad (58)$$

This is automatic to lowest order in perturbation theory, where $a m_{\mathcal{R}}^{div} \sim C_{\mathcal{R}}$, remembering that the Casimirs satisfy (32). This also ensures that the perturbative expression for the renormalized Polyakov loop, (55), is well behaved at large N .

McLerran and Svetitsky [4] used the expectation value of a loop to define the free energy of a test quark. If this test free energy is defined from the renormalized loop as $\mathcal{F}_{\mathcal{R}} = -T \log(|\langle \tilde{\ell}_{\mathcal{R}} \rangle|)$, then while it is positive near T_d , from (55) it is negative at high temperature, $\mathcal{F}_{\mathcal{R}} \sim -C_{\mathcal{R}} T / \log(T)^{3/2}$.

While the divergent masses depend upon the ultraviolet cutoff in a unremarkable manner, the renormalization constants are not like those of local operators. In four spacetime dimensions, the renormalization constants of local operators are independent of temperature. In contrast, the renormalization constants of Polyakov loops are temperature dependent, but just because the length of the path for a Polyakov loop is $1/T$.

Renormalization implies that the only measurable quantities are single traces of Wilson lines. Consider the most general, gauge invariant combination of bare Wilson lines possible. For example, start with $\text{tr } \mathbf{L}_{\mathcal{R}_1^+}^{q_1^+}$, which represents the propagator for a test quark, in the representation \mathcal{R}_1^+ , q_1^+ times around some fixed loop in spacetime. Generically, we can take powers of this trace, and then multiply different powers of different traces together. We can also do the same with conjugate operators. By the character expansion [53], any such combination can be reduced to a linear sum over traces of single Wilson lines in different, irreducible representations:

$$\begin{aligned} & \left(\text{tr } \mathbf{L}_{\mathcal{R}_1^+}^{q_1^+} \right)^{n_1^+} \left(\text{tr } \mathbf{L}_{\mathcal{R}_2^+}^{q_2^+} \right)^{n_2^+} \dots \left(\text{tr } (\mathbf{L}^\dagger)_{\mathcal{R}_1^-}^{q_1^-} \right)^{n_1^-} \dots \\ &= \sum_{\mathcal{R}} c_{\mathcal{R}} \ell_{\mathcal{R}} = \sum_{\mathcal{R}} c_{\mathcal{R}} \mathcal{Z}_{\mathcal{R}} \tilde{\ell}_{\mathcal{R}}. \end{aligned} \quad (59)$$

Here all n 's and q 's are positive integers; the constants $c_{\mathcal{R}}$, and the representations \mathcal{R} which one must sum over, are determined by group theory [53]. Because irreducible representations form a complete basis over all $SU(N)$ representations [53], we can insist that only linear powers of Wilson lines appear on the right hand side. With a linear sum, renormalization is then just a matter of replacing bare by renormalized loops.

Assuming that all $m_{\mathcal{R}}^{div} > 0$, (57), so the $\mathcal{Z}_{\mathcal{R}}$ all vanish as $a \rightarrow 0$, in the continuum limit only the identity representation survives. This is of no physical consequence: the physical quantities, the traces of renormalized Wilson lines, are hidden in the corrections to this relation, which are exponential in $1/a$ as $a \rightarrow 0$.

This was discovered numerically. To a high accuracy, we found that $\langle |\ell_3|^2 \rangle \approx 1/9$; corrections varied from $\sim 7\%$ for $N_t = 4$, to $\sim .2\%$ for $N_t = 10$. This is because from (19), $\langle |\ell_3|^2 \rangle - 1/9 \approx 8\mathcal{Z}_8 \langle \tilde{\ell}_8 \rangle / 9$; because of the octet renormalization constant, \mathcal{Z}_8 , this is a small quantity.

Previous work on the renormalization of loops at zero temperature concentrated on loops in the fundamental and adjoint representations, especially on the case of loops with cusps [35, 36]. The case of traces of lines which wrap around the same loop several times, or products of such traces, was neglected. At nonzero temperature, though, the natural loops to consider are those at the same point in space, wrapping around in imaginary time in all possible ways. As discussed, this is equivalent to the set of loops which wrap around in imaginary time just once, although in arbitrary representations.

III. LATTICE MEASUREMENTS OF $SU(3)$ POLYAKOV LOOPS

A. General Method

We turn to the case of three colors. Group theory tells us how bare loops are related, through expressions such as (39). After renormalization, we do not know how renormalized loops are related. Except at very high temperature, where we can use perturbation theory, (55), the only way to compute renormalized loops is through numerical simulations on the lattice.

In this section we discuss how we extract renormalized Polyakov loops for the lowest, nontrivial representations of $SU(3)$ color. Consider a lattice with N_s steps in each of the three spatial directions, and N_t steps in the time direction. At lattice spacing a , the physical temperature $T = 1/(aN_t)$. As discussed in the Introduction, to extract the mass divergence, we consider a series of lattices, all at the same temperature, but with different values of the lattice spacing, a , and so N_t ; N_s/N_t is kept in fixed ratio. At a given value of T/T_d , we assume that the logarithm of the expectation value of a single, bare Polyakov loop can be written as a power series in $1/N_t$:

$$- \log \langle \ell_{\mathcal{R}} \rangle = f_{\mathcal{R}}^{div} N_t + f_{\mathcal{R}}^{ren} + f_{\mathcal{R}}^{lat} \frac{1}{N_t}. \quad (60)$$

In four spacetime dimensions, $f_{\mathcal{R}}^{div} = am_{\mathcal{R}}^{div}$. (In three dimensions, the series is $f_{\mathcal{R}}^{div} \log(N_t) + f_{\mathcal{R}}^{ren} + f_{\mathcal{R}}^{lat}/N_t$.)

Each of the $f_{\mathcal{R}}$'s is a power series in the coupling constant, g^2 . On the lattice, this is a series in the bare coupling constant, and becomes, in the continuum limit, a series in the renormalized coupling constant. As such, the $f_{\mathcal{R}}$'s are functions only of the temperature divided by the renormalization mass scale; or equivalently, of T/T_d . By comparing expectation values at the same temperature, but different values of N_t , we can extract $am_{\mathcal{R}}^{div}$. What remains is the renormalized loop in the continuum limit,

$$\langle \tilde{\ell}_{\mathcal{R}} \rangle = \exp(-f_{\mathcal{R}}^{ren}). \quad (61)$$

There are also corrections at finite lattice spacing, $f_{\mathcal{R}}^{lat}$. Near the continuum limit, these effects begin at $1/N_t$, with $f_{\mathcal{R}}^{lat} = \sum_{j=1}^{\infty} c_j/N_t^{j-1}$. In weak coupling, $c_1 \sim g^4$; these are corrections to the one loop term on the lattice, after resumming the Debye mass. Corrections in $c_2 \sim g^5$ presumably arise as lattice corrections to the continuum term, (61).

As is common on the lattice, we work at a fixed ratio of N_s/N_t . Thus we implicitly assume that the dependence upon this ratio is negligible in the infinite volume limit. This can be studied analytically, but requires a careful treatment of the constant modes. A perturbative study is given by Heller and Karsch, especially Sec. (4.4) [37]. For now, we defer this question for future study [55].

B. Lattice Results

In practice, our method is not quite so trivial. The difficulty is that if we require the comparison lattices to have the same physical temperature, but different N_t , then the deconfining transition occurs at different values of the lattice coupling constant. This significantly complicates the analysis.

In the simulations, the Wilson lattice action was used, with lattice coupling constant $\beta = 6/g^2$. The number of time steps taken were $N_t = 4, 6, 8$, and 10. The number of steps in the spatial direction, N_s , was always kept fixed at $N_s = 3N_t$; we did not study what happens as this ratio is varied. The value of the coupling constant at which the deconfining transition occurs, β_d , was determined by monitoring the peak in the susceptibility of the triplet loop, to give the values in Table I.

By using non-perturbative renormalization [28], the relationship between β and the temperature was found to be:

$$\begin{aligned} \log \frac{T}{T_d} = & 1.7139 (\bar{\beta} - \bar{\beta}_d) - 0.8155 (\bar{\beta}^2 - \bar{\beta}_d^2) \\ & + 0.6667 (\bar{\beta}^3 - \bar{\beta}_d^3), \end{aligned} \quad (62)$$

where $\bar{\beta} \equiv \beta - 6$ and $\bar{\beta}_d \equiv \beta_d - 6$. In terms of physical temperature, our lattices varied from $\approx .5T_d$ to $\approx 3T_d$.

TABLE I: The lattice coupling constant for the deconfining transition, β_d , at different time steps.

N_t	β_d
4	5.690(5)
6	5.89(1)
8	6.055(6)
10	6.201(5)

The lattice calculation was done using the over relaxed Cabibo-Marinari pseudo-heatbath algorithm. Each update step contained 4 heatbath updates and six overrelaxation steps. A measurement was performed every 10 update steps. In Table II we summarize our statistics in each case. Our lattice data for the bare Polyakov loops are presented in Tables III, IV, V, and VI. They are also plotted in Figures 2, 3, 4, and 5.

TABLE II: .

N_t	Measurements
4	10000
6	400
8	400
10	400

TABLE III: Bare Polyakov loops for $N_t = 4$.

β	$\langle \ell_3 \rangle$	$\langle \ell_6 \rangle$	$\langle \ell_8 \rangle$	$\langle \ell_{10} \rangle$
5.50	0.0104(22)	0.0037(9)	0.0020(6)	0.0024(5)
5.60	0.01659(9)	0.003636(19)	0.002522(19)	0.002139(11)
5.65	0.02456(14)	0.003696(19)	0.002670(21)	0.002126(11)
5.69	0.0854(5)	0.00588(4)	0.00726(6)	0.002202(12)
5.70	0.1233(4)	0.00834(4)	0.01172(6)	0.002254(12)
5.75	0.17803(17)	0.01503(4)	0.02205(6)	0.002372(12)
5.80	0.19956(15)	0.01925(5)	0.02791(6)	0.002490(13)
5.90	0.22978(14)	0.02657(5)	0.03772(6)	0.002825(15)
6.00	0.25301(13)	0.03340(5)	0.04649(6)	0.003328(17)
6.10	0.27307(13)	0.04010(6)	0.05492(6)	0.003979(19)
6.20	0.29075(13)	0.04660(6)	0.06298(7)	0.004747(20)
6.30	0.30695(12)	0.05319(6)	0.07103(7)	0.005748(22)
6.40	0.32174(12)	0.05964(6)	0.07880(7)	0.006821(24)

As the relationship between the lattice coupling constant and the physical temperature, (62) is nonlinear, it is not automatic ensuring that the temperature is the same when N_t changes. Thus we resort to interpolation, measuring the loops on a fixed grid, in β , for each N_t . For $N_t = 4, 6$, and 8 we have linearly interpolated the Polyakov loop values to the T/T_d values at which the measurements for $N_t = 10$ were done. Then, for each value of T/T_d , the expectation value of the bare Polyakov loop was fit to (60) — (61).

TABLE IV: Bare Polyakov loops for $N_t = 6$.

β	$\langle \ell_3 \rangle$	$\langle \ell_6 \rangle$	$\langle \ell_8 \rangle$	$\langle \ell_{10} \rangle$
5.70	0.00592(16)	0.00197(5)	0.00131(5)	0.00115(3)
5.80	0.00963(26)	0.00195(5)	0.00143(6)	0.00116(3)
5.82	0.0111(3)	0.00191(5)	0.00139(5)	0.00117(3)
5.84	0.0125(3)	0.00195(5)	0.00135(5)	0.001126(29)
5.86	0.0183(5)	0.00210(5)	0.00132(5)	0.001148(28)
5.88	0.0314(9)	0.00205(5)	0.00150(6)	0.00116(3)
5.89	0.0391(10)	0.00195(5)	0.00183(7)	0.00121(3)
5.90	0.0545(9)	0.00217(6)	0.00231(8)	0.001144(29)
5.92	0.0702(6)	0.00254(6)	0.00296(9)	0.00119(3)
5.95	0.0816(5)	0.00268(7)	0.00397(9)	0.00118(3)
6.00	0.0935(5)	0.00346(8)	0.00508(10)	0.00117(3)
6.10	0.1128(4)	0.00480(9)	0.00759(11)	0.00126(3)
6.20	0.1301(4)	0.00654(9)	0.01038(11)	0.00120(3)
6.30	0.1445(4)	0.00837(10)	0.01314(11)	0.00127(3)
6.40	0.1581(4)	0.01031(10)	0.01604(13)	0.00124(3)
6.50	0.1707(4)	0.01241(11)	0.01901(12)	0.00128(3)
6.60	0.1829(4)	0.01462(12)	0.02216(14)	0.00136(4)
6.70	0.1954(4)	0.01718(12)	0.02565(14)	0.00144(4)

TABLE V: Bare Polyakov loops for $N_t = 8$.

β	$\langle \ell_3 \rangle$	$\langle \ell_6 \rangle$	$\langle \ell_8 \rangle$	$\langle \ell_{10} \rangle$
5.80	0.00339(9)	0.00133(4)	0.00083(3)	0.000775(20)
5.90	0.00421(11)	0.00122(3)	0.00086(3)	0.000770(20)
6.00	0.00668(18)	0.00124(3)	0.00087(3)	0.000763(20)
6.02	0.00858(26)	0.00126(4)	0.00082(3)	0.000775(20)
6.04	0.0159(5)	0.00121(3)	0.00095(4)	0.000754(19)
6.06	0.0209(5)	0.00129(3)	0.00092(3)	0.000713(17)
6.08	0.0345(4)	0.00129(3)	0.00099(4)	0.000751(20)
6.10	0.0391(3)	0.00126(4)	0.00108(4)	0.000755(20)
6.15	0.04762(26)	0.00138(4)	0.00131(5)	0.000754(20)
6.20	0.05400(25)	0.00146(4)	0.00164(5)	0.000724(20)
6.30	0.06541(24)	0.00164(5)	0.00228(6)	0.000768(21)
6.40	0.07540(24)	0.00194(5)	0.00305(6)	0.000751(19)
6.50	0.08501(22)	0.00249(5)	0.00407(5)	0.000804(18)
6.60	0.09492(24)	0.00299(5)	0.00502(6)	0.000765(19)
6.70	0.10490(24)	0.00375(5)	0.00635(6)	0.000766(21)
6.80	0.11377(25)	0.00450(6)	0.00757(6)	0.000819(20)
6.90	0.12214(24)	0.00540(5)	0.00886(7)	0.000778(20)

In our measurements, we see no statistically significant term $\sim 1/N_t$, $f_{\mathcal{R}}^{lat} \approx 0$. Such terms will presumably be revealed by more precise measurements. The success of a fit to (60) indicates that on the lattice, the divergent mass $m_{\mathcal{R}}^{div}$ does exponentiate.

We stress that we make no assumptions about any of the functions $f_{\mathcal{R}}$. At a given value of the temperature, the logarithm of the expectation value of the bare loop, $\log(\langle \ell_{\mathcal{R}} \rangle)$, is a power series in $1/N_t$, beginning as $\sim N_t$, (60) — (61). Given the lattice data, for loops at the same

TABLE VI: Bare Polyakov loops for $N_t = 10$.

β	$\langle \ell_3 \rangle$	$\langle \ell_6 \rangle$	$\langle \ell_8 \rangle$	$\langle \ell_{10} \rangle$
6.00	0.00272(9)	0.00088(3)	0.00058(3)	0.000525(18)
6.10	0.00362(13)	0.00085(3)	0.00064(4)	0.000537(22)
6.15	0.00524(15)	0.000904(24)	0.000588(23)	0.000560(13)
6.18	0.00672(16)	0.000906(18)	0.000615(17)	0.000550(11)
6.20	0.00839(27)	0.000909(23)	0.000633(24)	0.000512(14)
6.22	0.01651(22)	0.000927(18)	0.000627(18)	0.000561(11)
6.25	0.02167(17)	0.000929(18)	0.000641(18)	0.000532(11)
6.30	0.02741(22)	0.00091(3)	0.00070(4)	0.000537(18)
6.40	0.03444(24)	0.00092(4)	0.00084(4)	0.000555(21)
6.50	0.04142(24)	0.00092(4)	0.00099(4)	0.000521(20)
6.60	0.04861(18)	0.00098(3)	0.00111(4)	0.000543(17)
6.70	0.05505(18)	0.00118(3)	0.00146(5)	0.000511(17)
6.80	0.06204(19)	0.00128(4)	0.00193(5)	0.000549(16)
6.90	0.06852(19)	0.00154(3)	0.00255(5)	0.000555(16)
6.95	0.07130(18)	0.00152(3)	0.00270(4)	0.000546(15)

physical temperature and different values of N_t , there is nothing left over to adjust.

In Fig. 6 we present a typical fit for the expectation value of the bare triplet loop. It is clear that the bare loop decreases, with increasing N_t , for all temperatures measured.

In Table VII, we give the expectation values of the bare Polyakov loops for different representations. We chose the smallest N_t , $N_t = 4$, where the signals are greatest. For reference, we also include the Casimirs of the different representations.

TABLE VII: Approximate expectation values of the bare Polyakov loop, and Casimirs, for $N_t = 4$ and $T = 2T_d$.

\mathcal{R}	$\langle \ell_{\mathcal{R}} \rangle$	$C_{\mathcal{R}}$
3	.25	4/3
8	.04	3
6	.035	10/3
10	.004	6

For all representations, the signal decreases with increasing N_t . This indicates that every $am_{\mathcal{R}}^{div}$ is positive, as suggested before, (57). We were only able to measure a signal for the decuplet loop on the smallest lattice, $N_t = 4$. Perhaps a modified Polyakov loop, as discussed in the Appendix, might help. We do not discuss the decuplet loop further.

Fig. 7 shows our results for the product of the lattice spacing times the divergent mass, $am_{\mathcal{R}}^{div}$. For the triplet loop, this product doesn't vary much with temperature, but those for the sextet and octet loops do. At the highest temperature, $\approx 3T_d$, the values are approximately what one expects from lowest order in perturbation theory, where the divergent masses scale like the Casimir of the representation, $am_{\mathcal{R}}^{div} \sim C_{\mathcal{R}}$, (50). As

the temperature decreases below $\approx 1.5T_d$, though, the perturbative ordering of $am_6^{div} > am_8^{div}$ is reversed, with $am_8^{div} > am_6^{div}$. All divergent masses are approximately equal below T_d , although the signals are poor.

After dividing by the renormalization constant, we obtain the renormalized loops of Fig. 8. Below T_d , the triplet and sextet fields, which carry $Z(3)$ charge, should vanish in the infinite volume limit. What is striking is that below T_d , the $Z(3)$ neutral adjoint loop — which could be nonzero — is also too small for us to measure:

$$\langle \tilde{\ell}_8 \rangle \approx 0 \quad , \quad T < T_d. \quad (63)$$

Previous studies found this for bare adjoint loops on small lattices, such as $N_t = 4$ [10, 27, 54, 56].

In the deconfined phase, the triplet loop is always greatest, followed by the octet, and then the sextet loop. At T_d^+ , the triplet loop jumps to a relatively large value, $\approx .4$, although the exact value is not very well determined. Due to the increase in correlation lengths, there is critical slowing down near T_d , and much more careful studies are required.

We then computed the expectation value of the difference between the sextet and octet loops, and their large N limit, (8) and (9). The results are presented in Fig. (9). Numerically, we find that both difference loops are negative. They each look like a “spike” down, with a maximum near T_d . The sextet spike is larger, $|\delta\tilde{\ell}_6| \leq .25$, with a maximum at $\approx 1.25T_d$. The octet spike is smaller, $|\delta\tilde{\ell}_8| \leq .2$, with a maximum nearer T_d , at $\approx 1.1T_d$. The octet spike falls off much more quickly than the sextet spike with increasing temperature: by $\approx 1.5T_d$, the octet difference vanishes, while the sextet difference persists all of the way to $\approx 3T_d$.

The most important feature of the difference loops is their overall magnitude: each is significantly smaller than one. As discussed in the Introduction, this indicates that factorization, which is exact for $N = \infty$, is approximately correct for $N = 3$. The difference loops will be discussed further in the next section.

We conclude this section by contrasting our method for determining renormalized Polyakov loops with that of Kaczmarek *et al.* [39]. They measure $\langle \ell_3(\vec{x})\ell_3(0) \rangle - |\langle \ell_3 \rangle|^2$, and extract \mathcal{Z}_3 by comparing with perturbation theory at short distances. Thus they need to measure two-point functions, although at just one value of N_t . We only need to measure one-point functions, but must do so at several values of N_t . Our results agree approximately with theirs; near T_d , we both have $|\langle \tilde{\ell}_3 \rangle| \approx .4$. It disagrees in that by $3T_d$, their $|\langle \tilde{\ell}_3 \rangle| \approx 1.0$, while ours is $\approx .9$. We do not know the reason for the differences between our results, although it could simply be due to the effects of finite lattice spacing.

IV. MATRIX MODELS FOR RENORMALIZED LOOPS

A. Effective Theories

We now discuss various effective models for the deconfining phase transition [5, 6, 7, 8, 9, 10, 11, 12, 13, 14, 15, 16, 17, 18, 19, 20, 21, 22, 23, 43, 44, 45, 46, 47, 48, 49, 50, 51, 54], and fit the renormalized triplet loop to a simple matrix model [47, 49, 54]. We then discuss the Gross–Witten point at large N , and how it may be related to three colors.

Numerical simulations on the lattice suggest that the transition is of second order for two colors [56] and of first order for three [24], four [26, 27], and six [27] colors. Lucini, Teper, and Wenger [27] present evidence that the latent heat grows $\sim N^2$ for these values of N . From this we presume that the transition is of first order for all $N \geq 3$. Arguments for a first order transition at infinite N have also been given by Gocksch and Neri [42].

We start with an effective lattice theory in the purely spatial dimensions. The actual value of the lattice spacing is irrelevant: all that matters is that it is much smaller than any physical length scale. Thus we concentrate on the region near T_d , and ignore $T \rightarrow \infty$.

The simplest approach is to follow Svetitsky and Yaffe [5], and construct an effective theory just for the Polyakov loop in the fundamental representation. This is certainly fine if the transition is of second order, as the only critical field should be that for the fundamental loop. For the second order transition of two colors, this predicts that the universality class is that of the Ising model, in agreement with the observed critical exponents [56]. For three colors, because $Z(3)$ symmetry allows a cubic invariant, this approach also predicts that the transition is invariably of first order. For more than three colors, though, it is not clear why the transition should be of first order. It would be if the interactions of the $Z(N)$ spins were like those of a Potts model, but they are not at high temperature [21]. Loops in higher representations can be introduced into this model, as new types of $Z(N)$ spins. However, at large N factorization does not follow naturally, but must be imposed by hand.

A variant of this approach is the Polyakov loop model [18, 19, 20, 21]. This starts with a potential for the (renormalized) fundamental loop, and assumes that the pressure is correlated to the value of the potential at its minimum. We presume that the same holds for the potential of the matrix model, secs. IV.B and IV.C.

The closest model to the underlying gauge theory is a gauged, nonlinear sigma model for the Wilson line \mathbf{L}_N [6, 18]. In such a model, Higgs phases, in which the $SU(N)$ symmetry is spontaneously broken, can appear, but these are not expected to arise if there are no dynamical scalars about. Remember that deconfinement is not a Higgs effect: only $Z(N)$ is broken in the deconfined phase, not $SU(N)$.

Assuming that Wilson lines form the essential degrees

of freedom in the effective theory, we take as the partition function:

$$\mathcal{Z} = \int \Pi d\mathbf{L}_N(i) \exp(-\mathcal{S}(\ell_{\mathcal{R}}(i))) ; \quad (64)$$

i denotes lattice sites in the spatial directions. We assume that only Polyakov loops enter into the effective action, and consider only constant solutions in mean field theory. We neglect all kinetic terms, including those for the Wilson line, Polyakov loops, and color magnetic fields [17]. The effects of fluctuations, which are controlled by these kinetic terms, can be important, especially in three spacetime dimensions [60].

At each site, the measure in (64) implicitly contains a constraint to enforce that $\mathbf{L}_N(i)$ is a $SU(N)$ matrix. As such, loops $\ell_{\mathcal{R}}(i)$ are constructed by the usual relations of group theory. This is most convenient, since then all loops automatically have the right $Z(N)$ charge, and satisfy factorization at large N . Moreover, at each site we can use the character expansion, (59), to reduce any product of loops to a linear sum. This vastly restricts the number of possible couplings which can arise.

In a sigma model over a symmetric space, the trace of \mathbf{L}_N is everywhere some fixed constant [38]. In the present instance, however, the trace of the Wilson line is not constant. Thus the action also includes a potential for the Wilson line [18]. Requiring the action to be $Z(N)$ invariant, this is a sum over Polyakov loops with vanishing $Z(N)$ charge:

$$\mathcal{W} = N^2 \sum_i \sum_{\mathcal{R}}^{e_{\mathcal{R}}=0} \gamma_{\mathcal{R}} \ell_{\mathcal{R}}(i) ; \quad (65)$$

the $\gamma_{\mathcal{R}}$ are coupling constants. This series begins with the adjoint loop.

Next, loops on one site can interact with those on another site:

$$\mathcal{S}_{\mathcal{R}} = -\frac{N^2}{3} \sum_{i,\hat{n}} \sum_{\mathcal{R},\mathcal{R}'}^{e_{\mathcal{R}}+e_{\mathcal{R}'}=0} \beta_{\mathcal{R},\mathcal{R}'} \text{Re} \ell_{\mathcal{R}}(i) \ell_{\mathcal{R}'}(i+\hat{n}) . \quad (66)$$

Re denotes the real part, and $\beta_{\mathcal{R},\mathcal{R}'} = \beta_{\mathcal{R}',\mathcal{R}}$. We just write nearest neighbor interactions, given by the sum over the lattice vector \hat{n} , but this is inessential. The sum over representations is restricted by the requirement that the total $Z(N)$ charge of each term is zero, modulo N . There are both diagonal couplings, where \mathcal{R}' is the representation conjugate to \mathcal{R} , and off-diagonal couplings, where $\mathcal{R}' \neq \mathcal{R}^*$. This is the complete set of independent couplings.

B. Mean Field and Matrix Models for $N = 3$

For three colors, the simplest action includes just the triplet loop [48]

$$\mathcal{S}_3 = -3\beta_3 \sum_{i,\hat{n}} \text{Re} \ell_3(i) \ell_3^*(i+\hat{n}) ; \quad (67)$$

$\beta_{3,3^*} \equiv \beta_3$. We use this to develop a mean field approximation, replacing all nearest neighbors by an average

value. On a cubic lattice in three dimensions, if the value of each neighboring spin is $\ell_0 = \langle \ell_3 \rangle$ in (67), the partition function of (64) reduces to one for a single site,

$$\mathcal{Z} = \int d\mathbf{L}_3 \exp(+18\beta_3 \ell_0 \text{Re} \ell_3) \equiv \exp(-9\mathcal{V}) . \quad (68)$$

This is a matrix model, but one whose coupling constant depends on the value of the condensate, ℓ_0 . We introduce the single site potential, \mathcal{V} . The mean field condition is that the average value, computed with this action, is equal to the assumed value [38]:

$$\ell_0 = -\frac{1}{2\beta_3} \frac{\partial}{\partial \ell_0} \mathcal{V} . \quad (69)$$

As \mathbf{L}_N is an $SU(N)$ matrix, it is the unitary transformation of a diagonal matrix, with $N-1$ independent eigenvalues. When $N=2$, the integral like (68) is elementary, and can be evaluated in terms of Bessel functions. These can also be done when $N>2$, but we found it easier to simply evaluate it numerically. Explicitly, with $\mathbf{L}_3 = U \text{diag}(\exp(i\theta_1), \exp(i\theta_2), \exp(-i(\theta_1+\theta_2))) U^\dagger$, the normalized Haar measure, including the van der Monde determinant, is

$$d\mathbf{L}_3 = \frac{1}{3\pi^2} (1 - \cos(\theta_1 - \theta_2))(1 - \cos(2\theta_1 + \theta_2)) (1 - \cos(\theta_1 + 2\theta_2)) d\theta_1 d\theta_2 . \quad (70)$$

This mean field theory was studied in the context of the deconfinement transition by several groups [47, 48, 49, 54]. Like the lattice data, the transition is of second order for $N=2$, and first order when $N \geq 3$. For three colors, Damgaard [54] used eq. (69) to compute the expectation value of the triplet loop; expectation values for the sextet, adjoint and decuplet loops were then computed from that. Damgaard compared the results of this mean field theory to lattice data for bare Polyakov loops, with $N_t = 3$, by Markum, Faber, and Meinhart [37], finding qualitative agreement.

We stress that the approximate agreement between this mean field theory, and lattice data at small N_t , is in some sense fortuitous. For small N_t , the $\mathcal{Z}_{\mathcal{R}}$ are not much different from one, and so the bare values are not far from the renormalized values; even so, they are not identical. To see this in another way, we computed the ratio of the difference loop, to the loop itself, for the bare octet loop: $|\langle \ell_8 \rangle - |\langle \ell_3 \rangle|^2| / \langle \ell_8 \rangle$. This ratio is $\sim 50\%$ at $N_t = 4$, and increases to $\sim 100-200\%$ for $N_t = 10$. This is to be compared with the values for the renormalized octet difference loop in fig. (4), which is $\leq 12\%$. Thus while renormalized loops satisfy factorization, bare loops do not.

In this vein, recently Dittmann, Heinzl, and Wipf computed the effective potential for bare doublet loops in a

pure $SU(2)$ gauge theory [23]. Because only renormalized loops satisfy factorization, we suggest that the effective potential for renormalized loops is much simpler than that for bare loops.

We next compare the solution of mean field theory, eq. (69), to our lattice data for the renormalized triplet loop. We find that a linear relationship between the mean field coupling constant, β_3 , and the temperature, T/T_d , is approximately valid. A least squares fit gives

$$\beta_3 = (0.46 \pm 0.02) + (0.33 \pm 0.02) \frac{T}{T_d}. \quad (71)$$

The computed coupling, as well as the fitted curve, is shown in Fig. 10. A quadratic term was included in the fit but the coefficient was found to be zero within the error bars. Significant deviations are seen at both the highest temperature, $\approx 3T_d$, and also at the two points closest to T_d ; see the discussion at the end of this subsection. The approximate linear relationship between β_3 and the temperature is typical of mean field theory for spin models [38].

Using this relationship between the mean field coupling and the temperature, we then computed mean field results for the sextet, octet, and decuplet loops. The comparison to our lattice data are shown in Fig. 11. Notice that although we could not extract from the lattice a signal for the decuplet loop, the mean field theory predicts that while the decuplet loop is less than the sextet, it is not that small; for example, $\ell_{10}(3T_d) \approx .4$.

To obtain a more precise measure of the quality of our fits, we computed the difference loops in our mean field approximation, and plot them in Fig. 12. We do this because even in this simple mean field approximation, there are corrections to $N = \infty$ factorization at $N = 3$. Now compare the difference loops in mean field theory, Fig. 12, to those from the lattice, Fig. 9. As expected from general arguments, the adjoint difference loop is always smaller than the sextet difference loop; also, both difference loops are negative in mean field theory. In detail, however, the difference loops found from mean field theory are very different from those found from the lattice. First, in magnitude the difference loops from mean field theory are at least a factor of three times smaller than found from the lattice. Further, their temperature dependence is very different: in mean field theory, both difference loops are greatest at about $\approx 1.5T_d$, with approximately the same width, $\pm .5T_d$. In contrast, the difference loops from the lattice have a maximum much closer to T_d ; while the sextet has a tail which persists to $\approx 3T_d$, the octet really appears to be a sharp, narrow spike.

The quality of the fit could be improved by including other terms in the action. We started by including an adjoint loop in the potential at each site, (65), $\sim \gamma_8 \ell_8$. Within our numerical accuracy, this only appeared to produce a shift in $\beta_3 \rightarrow \beta_3 + \gamma_8$. We show in the next section that this can be understood at infinite N .

To model the sextet and octet loops, it is necessary

to add corresponding fields at each site. In (66) there are two diagonal couplings, $\beta_{6,6^*}$ and $\beta_{8,8}$, and one off-diagonal coupling, $\beta_{3,6}$. Even in mean field theory, it is tedious to solve numerically for several, coupled condensates; the results of a more careful study will be presented separately [55].

The presence of other loops obviously feeds back into the triplet loop. One of the clearest tests of this is the value of the triplet loop at T_d . In a mean field theory which includes just the triplet loop, (69), numerically we estimate that $\ell_3(T_d) \approx .485 \pm .001$; this is consistent with the value of $\approx .49$ in [47]. This is significantly higher than the values of the renormalized loop from the lattice, where both we and [39] find $\ell_3(T_d) \approx .4$. In a $N = 3$ matrix model which includes both triplet and sextet loops, we find that the value of the triplet loop at T_d decreases significantly by adding $\beta_{3,6}$, as this represents a linear coupling between the two loops [55]. It is also possible to decrease $\ell_3(T_d)$ by adding a term for the decuplet loop to the potential \mathcal{W} with the appropriate sign [55].

Thus the approximate linearity in β_3 with T , (71), should be treated as preliminary. Further, we doubt that it is true for all couplings. In particular, since the octet difference loop is such a sharp, narrow spike in temperature, it appears that we can only model it with a β_8 which varies non-monotonically with temperature; *i.e.*, which is itself a spike. This is not so obvious for the sextet loop, due to the triplet-sextet mixing from the coupling $\beta_{3,6}$. The sextet loop is also affected by its coupling with itself, through the coupling $\beta_{6,6}$, and by the decuplet loop in the potential.

Nevertheless, the matrix model proposed in sec. IV.A appears to be a useful way of characterizing the condensates of renormalized Polyakov loops when $N = 3$ [55].

C. Matrix Models: $N > 3$

For general N , the simplest possibility is to start with an action including just the fundamental loop,

$$\mathcal{S}_N = -\frac{N^2}{6} \beta \sum_{i,\hat{n}} \text{Re } \ell_N(i) \ell_N^*(i + \hat{n}), \quad (72)$$

$\beta \equiv \beta_{N,N^*}$. For the action to be of order N^2 at large N , β must be of order one as $N \rightarrow \infty$. Positive values of β correspond to a ferromagnetic coupling. As the perturbative vacuum at high temperature is completely ordered, $\beta \rightarrow +\infty$ as $T \rightarrow \infty$. We assume $\beta > 0$ [61].

At infinite N , if the fundamental loop condenses, loops in higher representations are fixed by factorization. The condensate for the fundamental loop is determined by the potential, \mathcal{W} of (65).

We start with the mean field analysis of (72), following the discussion of Kogut, Snow, and Stone [47]. We then discuss how these results change when the potential \mathcal{W} , (65), is added [45, 46]. A similar discussion was given recently by Aharony *et al* [14].

Replacing the values of all nearest neighbors by an average value ℓ_0 , we need to evaluate the integral at one site,

$$\begin{aligned} \mathcal{Z} &= \int d\mathbf{L}_N \exp(N^2(2\beta\ell_0) \operatorname{Re} \ell_N) \\ &\equiv \exp(-N^2\mathcal{V}_{GW}(\beta\ell_0)) . \end{aligned} \quad (73)$$

The mean field condition is

$$\ell_0 = -\frac{1}{2\beta} \frac{\partial}{\partial \ell_0} \mathcal{V}_{GW}(\beta\ell_0) . \quad (74)$$

This condition is equivalent to minimizing the mean field potential

$$\mathcal{V}_{mf}(\beta, \ell) = \beta\ell^2 + \mathcal{V}_{GW}(\beta\ell) . \quad (75)$$

We replace ℓ_0 by ℓ , and interpret the result as a potential for ℓ . At a fixed β , as usual the vacuum ℓ_0 is given by minimizing \mathcal{V}_{mf} with respect to ℓ .

Since an overall factor of N^2 is scaled out of the potential, a nonzero value of $\mathcal{V}_{mf}(\ell_0)$ implies that the free energy $\sim N^2$. This is expected in the deconfined phase from the liberation of $\sim N^2$ gluons. In the confined phase, Thorn [10] noted that as all states are color singlets, their free energy is at most of order one, so $\mathcal{V}_{mf}(\ell_0) \sim 1/N^2 \approx 0$. This scaling also motivated the Polyakov loop model [18, 19, 20, 21]. Here, we assume that to go from the single site model to thermodynamics, we multiply \mathcal{V}_{mf} by T^4 times the volume of space.

The potential \mathcal{V}_{GW} has been computed in the large N limit by Gross and Witten [43]. At infinite N the result is nonanalytic, and is given by two *different* potentials. For small ℓ , the potential is just a mass term,

$$\mathcal{V}_{mf}^- = \beta(1 - \beta)\ell^2 \quad , \quad \ell \leq \frac{1}{2\beta} , \quad (76)$$

while at large ℓ , the potential is

$$\mathcal{V}_{mf}^+ = -2\beta\ell + \beta\ell^2 + \frac{1}{2} \log(2\beta\ell) + \frac{3}{4} \quad , \quad \ell \geq \frac{1}{2\beta} . \quad (77)$$

The physical interpretation of this potential is rather different from the context in which it arose. Gross and Witten considered a $U(N)$ lattice gauge theory in two dimensions, with lattice coupling constant $\beta_{GW} \equiv \beta\ell$ [43]. This is the only parameter in the model, and there is no condition to fix ℓ_0 . Instead, the expectation value of $\operatorname{Re} \ell_N$ is related to the string tension; it changes with β_{GW} , but is always nonzero. The two potentials in (76) and (77) correspond to weak and strong coupling branches of the free energy. About $\beta_{GW} = 1/2$, the first and second derivatives of the free energy are continuous, but the third derivative is not, so there is a third order phase transition in β_{GW} .

In mean field theory, β is an effective coupling for the fundamental loop. As a function of ℓ at fixed β , the

first and second derivatives of the potential are everywhere continuous, but third (and higher) derivatives are discontinuous at a single point, when $\ell = 1/(2\beta)$. This nonanalyticity is special to $N = \infty$: the mean field potential is everywhere continuous for finite N .

Overlooking this discontinuity, the potential \mathcal{V}_{mf} behaves as a potential should. When $\beta < 1$, the potential just increases monotonically with ℓ , so the minimum is at $\ell_0 = 0$. For $\beta > 1$, the potential about the origin is given by \mathcal{V}_{mf}^- , and so starts out with a negative mass term. The potential decreases with increasing ℓ , with a single minimum when

$$\ell_0 = \frac{1}{2} \left(1 + \sqrt{\frac{\beta - 1}{\beta}} \right) . \quad (78)$$

When $\ell > \ell_0$, the potential increases monotonically. For all β , the potential is bounded at large ℓ , $\mathcal{V}_{mf}^+ \sim +\beta\ell^2$ as $\ell \rightarrow \infty$. (For $\ell > 1/(2\beta)$, the extremal condition $\partial\mathcal{V}_{mf}^+/\partial\ell = 0$ is a quadratic equation. There is another root besides (78), but it occurs for $\ell < 1/(2\beta)$, and so doesn't matter.)

Thus there is a confined phase for $\beta < 1$, and a deconfined phase for $\beta > 1$. The expectation value of the loop, ℓ_0 , jumps from zero below the transition, $\beta = 1^-$, to $\frac{1}{2}$ just above, $\beta = 1^+$. The latter is (10) of the Introduction. In the limit $\beta \rightarrow \infty$, $\ell_0 \rightarrow 1$.

To verify that the transition is in fact of first order, consider the value of the potential at its minimum. In the confined phase, $\ell_0 = 0$, so $\mathcal{V}_{mf}^-(\ell_0) = 0$ for all $\beta < 1$, including $\beta \rightarrow 1^-$. In the deconfined phase, using (78) one finds that

$$\mathcal{V}_{mf}^+(\ell_0) \approx -\frac{\beta - 1}{4} + \dots , \quad (79)$$

as $\beta \rightarrow 1^+$. Thus the first derivative of $\mathcal{V}_{mf}(\ell_0)$, which respect to β , is discontinuous when $\beta = 1$.

If we assume that β is linear in the temperature — as found for three colors — then the deconfining transition is thermodynamically of first order at $N = \infty$, with a latent heat $\sim N^2$. In this we agree with [47].

Even so, the non-analyticity of the potential still has striking physical consequences. In particular, exactly at $\beta = 1$, the potential is completely *flat* for ℓ between 0 and $\frac{1}{2}$, $\mathcal{V}_{mf}^- = 0$ [63]. The potential then increases monotonically, starting out to cubic order in $\ell - \frac{1}{2}$. The only reason the order parameter can jump, despite the flatness of the potential, is because $\beta = 1$ is special: then, and only then, does the point at which the potential is discontinuous coincide with the nontrivial minimum.

To appreciate this in another way, consider how the mass squared, $m^2 = \partial^2\mathcal{V}_{mf}/\partial\ell^2$ changes. Approaching the transition in the confined phase implies that we compute about $\ell_0 = 0$,

$$m_-^2 \approx 2(1 - \beta) \quad , \quad \beta \rightarrow 1^- . \quad (80)$$

In contrast, approaching the transition in the deconfined phase, we compute about $\ell_0 = \frac{1}{2}$,

$$m_+^2 \approx 4\sqrt{\beta-1} \quad , \quad \beta \rightarrow 1^+ . \quad (81)$$

Thus while both masses vanish at $\beta = 1$, they vanish with different powers of $|\beta - 1|$.

The mass of the Polyakov loop is of physical significance in the underlying gauge theory [19, 20]. In coordinate space, the connected two point function of $\ell(\vec{x})$ is:

$$\langle \ell_N^*(\vec{x}) \ell_N(0) \rangle - |\langle \ell_N \rangle|^2 \sim \frac{\exp(-M|\vec{x}|)}{|\vec{x}|} \quad , \quad |\vec{x}| \rightarrow \infty . \quad (82)$$

In the confined phase, $M = \sigma/T$, where σ is the string tension. In the deconfined phase, one can define $M = 2m_{Debye}$, where m_{Debye} is a (gauge-invariant) Debye mass. Assuming that $M \sim m$, with mass dimensions made up by some other physical mass scale, such as the temperature, this mean field theory predicts that the string tension vanishes at the transition as [62]:

$$\sigma(T) \sim (T_d - T)^{1/2} \quad , \quad T \rightarrow T_d^- , \quad (83)$$

and the Debye mass, as

$$m_{Debye}(T) \sim (T - T_d)^{1/4} \quad , \quad T \rightarrow T_d^+ . \quad (84)$$

One might refer to this as a “critical” first order transition: at the transition, the order parameter jumps, but the masses vanish, asymmetrically.

We next include the effects of the potential, (65). We start with the simplest term, $\gamma_2 \neq 0$, which is the contribution of the adjoint loop to the potential. At large N , in mean field approximation we need to evaluate the integral

$$\begin{aligned} \tilde{Z} &= \int d\mathbf{L}_N \exp(N^2(2\beta\ell \operatorname{Re} \ell_N + \gamma_2 |\ell_N|^2)) \\ &\equiv \exp\left(-N^2 \tilde{\mathcal{V}}(\beta\ell, \gamma_2)\right) . \end{aligned} \quad (85)$$

The solution is [45, 46]:

$$\tilde{\mathcal{V}}(\beta\ell, \gamma_2) = \gamma_2 k^2 + \mathcal{V}_{GW}(\beta\ell + \gamma_2 k) ; \quad (86)$$

where k is a variable which one minimizes with respect to. The variation with respect to k enforces the condition that the expectation value of ℓ_N^2 satisfies factorization. Finally, the mean field solution is given by minimizing a potential with respect to ℓ and k :

$$\tilde{\mathcal{V}}_{mf}(\ell, k) = \beta\ell^2 + \gamma_2 k^2 + \mathcal{V}_{GW}(\beta\ell + \gamma_2 k) . \quad (87)$$

This is trivial to solve. Expanding about $k = \ell + \delta k$, for $\delta k = 0$, this reduces to the previous mean field potential, except that the coupling constant is shifted, $\beta \rightarrow \beta + \gamma_2$. Further, if ℓ is extremal with respect to this shifted

mean field, the term linear in δk also vanishes. This follows because the Gross–Witten potential is a function only of $\beta\ell$, and not of β and ℓ separately. As discussed previously, for $N = 3$ we discovered numerically that in mean field theory, we can shift the adjoint coupling away, $\beta \rightarrow \beta + \gamma_2$.

This is very different from lattice gauge theories in two dimensions, where β_{GW} and γ_2 represent independent coupling constants [45, 46]. Then β_{GW} and γ_2 can be varied irrespectively of each other, and one finds that the third order transition, in β_{GW} for $\gamma_2 = 0$, can become a first order transition in the plane of β_{GW} and γ_2 [45, 46].

The generalization to $\gamma_4 \neq 0$ is direct. One includes a constraint field for $|\ell|^2$ and then solves the constraint at $N = \infty$. The mean field coupling β is again shifted, $\beta \rightarrow \beta + \gamma_2 + \# \gamma_4 \ell_0^2$, but by an amount which depends on the condensate, ℓ_0 ; there are also additional potential terms, $\sim \gamma_4 \ell_0^4$. Consequently, $\gamma_4 \neq 0$ corresponds to a change in the potential. Aharony *et al.* [14] show that for $\gamma_4 \neq 0$, ordinary transitions appear to be generic. In particular, first order transitions have finite correlation lengths in both phases.

This remains the case for an arbitrary potential, \mathcal{W} . At large N , this is just a sum of powers of the fundamental loop:

$$\mathcal{W} = \Sigma_{i,m} \left(\gamma_{2m} (|\ell_N|^2)^m + \xi_{mN} \left((\ell_N)^{mN} + \text{c.c.} \right) \right) . \quad (88)$$

This is a typical potential for a scalar field $\ell_N \equiv \ell_N(i)$: the adjoint loop acts like a mass term, while the other terms are interactions of quartic and higher order, invariant under a global symmetry of $Z(N)$.

We define the Gross–Witten point as the transition for a potential which is just the adjoint loop. All other interactions are dropped: $\beta + \gamma_2 \neq 0$, with $\gamma_4 = \gamma_6 = \dots = \xi_N = \xi_{2N} = \dots = 0$.

The deconfining transition for three colors appears to be close to the Gross–Witten point of infinite N . For example, although the data are very limited [25], the decrease of the Debye mass near T_d does seem to be significantly sharper than for the string tension, as indicated by the different “critical exponent” in (84) versus (83). Exactly how close $N = 3$ is to the Gross–Witten point of $N = \infty$ can be characterized within matrix models [55]. Effects which are important for three colors include the contribution of the decuplet loop, which is like a cubic interaction for the triplet loop, and the mixing between the triplet and sextet loops, $\beta_{3,6}$ in (66).

Assuming that three colors is near the Gross–Witten point, we can explain why $Z(N)$ neutral fields have small expectation values in the confined phase, (63). In the confined phase, the potential is purely a mass term, as corrections to (76) begin with the baryon vertex, $\sim (\ell_N)^N$ [44, 47, 51]. This vertex induces $Z(N)$ neutral expectation values, but as noted by Goldschmidt [44], these are of order $\sim \exp(-N)$.

That $N = 3$ is close to the Gross–Witten point could be an accident of three colors. The lattice will tell us

if the deconfining transition for four or more colors is also close to the Gross–Witten point. The lattice finds a first order transition [26, 27], but the crucial tests are the value of the renormalized, fundamental loop at T_d^+ , and whether the string tension and the Debye mass decrease significantly near T_d .

If this is not found, the most probable scenario is just that the transition becomes more strongly first order with increasing N . We term the transition strongly first order if the value of the renormalized fundamental loop at T_d^+ is near unity. Then at the transition, deconfinement is not halfway, as it is at the Gross–Witten point, but nearly complete.

For such a strongly first order transition, neither the string tension, nor the Debye mass, would need to change much about T_d . Gocksch and Neri [42] argued that the “loop” string tension is constant for $T \leq T_d$. In a Nambu string model, though, a large d expansion shows that when the ordinary string tension vanishes at T_d , the loop string tension is still $\approx 87\%$ of its value at zero temperature [62]. We are unaware of lattice data on the loop string tension.

V. OUTLOOK

In this paper we presented a general analysis of the renormalization of Polyakov loops, and applied it to measure the simplest loops for three colors in four dimensions. These results led us to consider effective matrix models for the deconfining phase transition. There are clearly many avenues for future study.

For two colors, there will be two regions. About T_d , there is a critical region, controlled by universality of the second order transition [5], and in which factorization fails. This may then match onto a mean field region, where factorization is approximately valid.

For three colors, careful measurements of the renormalized loops, and associated masses, will sharply constrain the couplings of the effective matrix model [55]. We note that while we could not extract an expectation value for the renormalized decuplet loop from that for the bare loop, mean field theory indicates that it is significant.

Simulations should quickly show if for the deconfining transition for four or more colors is near the Gross–Witten point.

Considering theories other than $SU(N)$, Holland, Minkowski, Pepe, and Wiese [65] noted that in a pure $G(2)$ gauge theory, there is no center to the gauge group, and so no absolute measure of confinement. This is analogous, though, to $Z(N)$ neutral loops in $SU(N)$, for which we measured no signal below T_d . In the simplest mean field theory for a $G(2)$ gauge theory, presumably there is a first order transition, with a value for the fundamental loop at T_d^+ near $\frac{1}{2}$. Maybe like $SU(3)$, the “deconfining” transition in a $G(2)$ gauge theory is also near the Gross–Witten point.

The renormalization of Wilson lines implies that once

the divergent mass is known, *all* renormalized loops can be computed. We suggest that numerical simulations measure loops of different shapes, such as Polyakov loops with cusps, Fig. (1), and circular loops, as can be computed in supersymmetric theories [13].

In the end, however, what is most important is to measure renormalized Polyakov loops for theories with dynamical quarks. Our method for computing renormalized Polyakov loops is completely unaffected by the presence of dynamical quarks. Given the flavor independence found for the pressure [24], it would be striking if the values of renormalized Polyakov loops, with dynamical quarks, are found to be close to those of the pure gauge theory. For recent results, see [39].

Acknowledgements: The research of A.D. is supported by the BMBF and the GSI; Y.H. and R.D.P., by U.S. Department of Energy grant DE-AC02-98CH10886; J.T.L., by D.O.E. grant DE-FG02-97ER41027; K.O., by the RIKEN/BNL Research Center and D.O.E. grant DF-FC02-94ER40818. The numerical work was done on a cluster of workstations at Brookhaven National Laboratory using the publicly available MILC code. J.L. thanks P. Arnold and H. Thacker for useful discussions. R.D.P. thanks: R. Brower and C. P. Korthals-Altes, for emphasizing the importance of mixed actions in matrix models; M. Creutz, for numerous discussions on group theory and the lattice; P. Damgaard, for many discussions of his work; G. Korchemsky, for explaining loops with cusps; also, Y. Dokshitzer, N. Drukker, D. J. Gross, T. Heinzl, and S. Necco. R.D.P. and Y.H. thank P. Petreczky for discussions concerning Polyakov loops on the lattice.

APPENDIX: IMPROVED WILSON LINE

It is difficult extracting renormalized Polyakov loops in representations such as the decuplet, because the bare loop is suppressed by a small renormalization constant. In this Appendix we give a formal discussion of how to improve the Wilson line [57].

Our discussion applies to any Wilson line along a path $x^\mu(s)$, where s is the path length along the curve. As shown in sec. II, (13), the propagator for a test quark is proportional to the Wilson line. Consequently, we consider a generalized propagator, by adding an operator \mathcal{X} to the covariant derivative:

$$\left(\frac{d}{ds} - igA^\mu \dot{x}^\mu - \mathcal{X} \right) \mathcal{G}(s, s') = \delta(s - s'); \quad (\text{A.1})$$

where $\dot{x}^\mu = dx^\mu/ds$. The representation is denoted implicitly. Schematically, the solution to this equation is

$$\mathcal{G}(s, s') = \theta(s - s') \mathcal{P} \exp \left(\int (igA^\mu \dot{x}^\mu + \mathcal{X}) ds \right), \quad (\text{A.2})$$

with \mathcal{P} denoting path ordering. The solution to \mathcal{G} is schematic because of the path ordering, but it is easy to

understand the solution as a power series in \mathcal{X} , with each insertion of \mathcal{X} sandwiched between a Wilson line on both sides.

Any possible operator \mathcal{X} has a higher mass dimension than the gauge field, so we make up the dimensions with inverse powers of the ultraviolet cutoff, such as the lattice spacing a . The important thing is that \mathcal{X} respects the relevant symmetries. Gauge invariance requires that \mathcal{X} transforms homogeneously under gauge transformations, but that is simply done by using powers of the field strength tensor, $G_{\mu\nu}$. The operator must also be invariant under how we parameterize arc length, $s \rightarrow s'(s)$. The final symmetry is the zig-zag symmetry of Polyakov [66]; for reparameterizations which go in the opposite direction, with $ds/ds' < 0$, \mathcal{X} should change sign.

The simplest possibility is

$$\mathcal{X} = a^2 g^2 G_{\mu\nu}^2 \sqrt{\dot{x}^2}. \quad (\text{A.3})$$

This is gauge covariant and reparameterization invariant, but is not zig-zag symmetric. If one abandons zig-zag symmetry, then this operator can be used to regularize the Wilson line, since it is just a field strength dependent “mass” term for the line.

One can satisfy all symmetries with the following operator,

$$\mathcal{X} = ag G_{\mu\nu} \frac{\dot{x}^\mu \ddot{x}^\nu}{\dot{x}^2}, \quad (\text{A.4})$$

where $\ddot{x} = d^2 x^\mu / ds^2$. A similar operator was noted by Polyakov and Rytchikov [66]. Since it vanishes for a straight path, where $\ddot{x}^\mu = 0$, it doesn’t help to regularize the Wilson line. It is also problematic to continue to Minkowski spacetime, since it is singular on the light cone [66].

To define an operator which satisfies all of our requirements, we define a unit vector normal to the path,

$$\hat{n}_\mu \dot{x}^\mu = 0 \quad , \quad \hat{n}^2 = 1. \quad (\text{A.5})$$

For a given direction, we introduce the \hat{n} dependent operator

$$\mathcal{X}_{\hat{n}} = \kappa g G_{\mu\nu} \dot{x}^\mu \hat{n}^\nu. \quad (\text{A.6})$$

We then define a modified Wilson line as

$$\int d\Omega_{\hat{n}} \mathcal{P} \exp \left(\int (ig A_\mu \dot{x}^\mu + \mathcal{X}_{\hat{n}}) ds \right). \quad (\text{A.7})$$

The operator $\mathcal{X}_{\hat{n}}$ inserts the field strength tensor perpendicular to the path. We then integrate over all directions of the insertion, with $d\Omega_{\hat{n}}$ the normalized integral over \hat{n} , $\int d\Omega_{\hat{n}} = 1$. We obviously cannot integrate over all directions \hat{n} in the exponential, or the term would vanish, and so do so in the prefactor of the exponential. Zig-zag symmetry is maintained by integrating over all \hat{n} .

In perturbation theory, to lowest order $\mathcal{X}_{\hat{n}}$ generates new divergences. In three spatial dimensions, and including a Debye mass $m_D \sim gT$ in the propagator for A_0

[3], the leading divergence is

$$\sim \frac{g^2}{T} \int d\Omega_{\hat{n}} \int \frac{d^3 k}{(2\pi)^3} \left(\frac{-1 + a^2 \kappa^2 (\hat{n} \cdot \vec{k})^2}{k^2 + m_D^2} \right). \quad (\text{A.8})$$

We assume that the ultraviolet divergence is cutoff strictly at momenta $1/a$. The usual term is $\sim \int d^3 k / k^2 \sim 1/a$, and is of the same order as the new term, $\sim a^2 \int d^3 k \sim 1/a$. For $\kappa < 1/\sqrt{3}$, (A.8) is negative, while for $\kappa > 1/\sqrt{3}$, it is positive. If a more realistic cutoff is used, then the value of κ at which the sign changes will be different, but for large κ (and to leading order in g^2) bare loops are enhanced, not suppressed.

Following the procedure in sec. (II.D), from $\log(\langle \ell \rangle)$ we compute as power series in N_t . The term linear in N_t gives $\mathcal{Z}_{\mathcal{R}}$, with the renormalized loop given by the term independent of N_t . We argue that while the $\mathcal{Z}_{\mathcal{R}}$ are κ dependent, the renormalized loops are not, at least in perturbation theory. To lowest order in g^2 , for $\kappa = 0$ the renormalized loop arises from the correction from the Debye mass term, $\sim g^2(m_D^2)^{1/2}/T \sim g^3$, (55) [3]. This is non-analytic in the Debye mass, and arises because the leading term is only linearly divergent. For the κ -dependent term, the leading term is cubically divergent, so corrections are $\sim g^2 \kappa^2 a^2 m_D^2 / (aT) \sim g^4 \kappa^2 aT$; but this is $\sim 1/N_t$, and vanishes as $N_t \rightarrow \infty$. There is a non-analytic term at one higher order in momentum, but this is even smaller, $\sim g^2 \kappa^2 a^2 (m_D^2)^{3/2} / T \sim g^5 \kappa^2 (aT)^2 \sim 1/N_t^2$. It seems likely that this holds for any κ -dependent terms: they contribute to terms $\sim 1/(aT) \sim N_t$, or to lattice corrections $\sim 1/N_t$ or smaller, but not to terms in the continuum limit, $\sim N_t^0$. This analysis is special to four spacetime dimensions: in three dimensions, the κ dependent term is quadratically divergent, and has logarithmic corrections, as for $\kappa = 0$.

While zig-zag symmetric, the term added, $\mathcal{X}_{\hat{n}}$, is not a phase factor; the coupling κ must be real in order to enhance the bare loop. As the bare loop is not the trace of a unitary matrix, there is no bound on the renormalized loop, as for $\kappa = 0$, (56); when $\kappa \neq 0$, $\mathcal{Z}_{\mathcal{R}}$ can diverge in the continuum limit, instead of vanishing.

On the lattice, adding a field strength tensor at a point corresponds to stapling a plaquette, as the average over \hat{n} becomes a sum over the directions transverse to the path. To lowest order in κ , this modification is the same as the smearing of link variables proposed by the APE collaboration [57]. We suggest doing this not just to lowest order, but to all orders in κ . This is related to the stout links of Morningstar and Peardon [57]. The difficulty is that eventually the Wilson line is smeared over the entire lattice, which must then be cut off in some way. On the other hand, the usual problem with smeared links is the need to project back to an element of $SU(N)$, which is unnecessary here.

-
- [1] G. 't Hooft, Nucl. Phys. B **138**, 1 (1978); *ibid.* **153**, 141 (1979).
- [2] A. M. Polyakov, Phys. Lett. B **72**, 477 (1978); L. Susskind, Phys. Rev. D **20**, 2610 (1979).
- [3] E. Gava and R. Jengo, Phys. Lett. B **105**, 285 (1981).
- [4] L. D. McLerran and B. Svetitsky, Phys. Rev. D **24**, 450 (1981).
- [5] B. Svetitsky and L. G. Yaffe, Nucl. Phys. B **210**, 423 (1982).
- [6] T. Banks and A. Ukawa, Nucl. Phys. B **225**, 145 (1983).
- [7] J. O. Andersen and M. Strickland, [arXiv:hep-ph/0404164]; J. P. Blaizot, E. Iancu and A. Rebhan, [arXiv:hep-ph/0303185]; U. Kraemmer and A. Rebhan, Rep. Prog. Phys. **67**, 351 (2004) [arXiv:hep-ph/0310337];
- [8] E. V. Shuryak and I. Zahed, [arXiv:hep-ph/0307267]; G. E. Brown, C. H. Lee, M. Rho and E. Shuryak, [arXiv:hep-ph/0312175]; E. V. Shuryak and I. Zahed, [arXiv:hep-ph/0403127].
- [9] N. Cabibbo and G. Parisi, Phys. Lett. B **59**, 67 (1975); J. J. Atick and E. Witten, Nucl. Phys. B **310**, 291 (1988); J. Hallin and D. Persson, Phys. Lett. B **B429**, 232 (1998) [arXiv:hep-ph/9803234]; B. Sundborg, Nucl. Phys. B **573**, 349 (2000) [arXiv:hep-th/9908001].
- [10] C. B. Thorn, Phys. Lett. B **99**, 458 (1981); J. Greensite and M. B. Halpern, Phys. Rev. D **27**, 2545 (1983); R. D. Pisarski, *ibid.* **29**, 1222 (1984); P. H. Damgaard, Phys. Lett. B **183**, 81 (1987); J. Polchinski, Phys. Rev. Lett. **68**, 1267 (1992) [arXiv:hep-th/9109007].
- [11] J. M. Maldacena, Adv. Theor. Math. Phys. **2**, 231 (1998) [Int. J. Theor. Phys. **38**, 1113 (1999)] [arXiv:hep-th/9711200]; S. S. Gubser, I. R. Klebanov and A. M. Polyakov, Phys. Lett. B **428**, 105 (1998) [arXiv:hep-th/9802109]; E. Witten, Adv. Theor. Math. Phys. **2**, 253 (1998) [arXiv:hep-th/9802150]; J. M. Maldacena, Phys. Rev. Lett. **80**, 4859 (1998) [arXiv:hep-th/9803002]; S. S. Gubser, I. R. Klebanov and A. A. Tseytlin, Nucl. Phys. B **534**, 202 (1998) [arXiv:hep-th/9805156]; A. Fotopoulos and T. R. Taylor, Phys. Rev. D **59**, 061701 (1999) [arXiv:hep-th/9811224]; O. Aharony, S. S. Gubser, J. M. Maldacena, H. Ooguri and Y. Oz, Phys. Rep. **32**, 183 (2000) [arXiv:hep-th/9905111]; J. Maldacena, [arXiv:hep-th/0309246].
- [12] E. Witten, Adv. Theor. Math. Phys. **2**, 505 (1998) [arXiv:hep-th/9803131]; O. Aharony and E. Witten, Jour. High Energy Phys. **9811**, 018 (1998) [arXiv:hep-th/9807205].
- [13] N. Drukker, D. J. Gross and H. Ooguri, Phys. Rev. D **60**, 125006 (1999) [arXiv:hep-th/9904191]; J. K. Erickson, G. W. Semenoff and K. Zarembo, Nucl. Phys. B **582**, 155 (2000) [arXiv:hep-th/0003055]; N. Drukker and D. J. Gross, Jour. Math. Phys. **42**, 2896 (2001) [arXiv:hep-th/0010274]; K. Zarembo, Nucl. Phys. B **643**, 157 (2002) [arXiv:hep-th/0205160].
- [14] O. Aharony, J. Marsano, S. Minwalla, K. Papadodimas, and M. Van Raamsdonk, [arXiv:hep-th/0310285];
- [15] K. Furuuchi, E. Schreiber, and G. Semenoff, [arXiv:hep-th/0310286];
- [16] H. J. Schnitzer, [arXiv:hep-th/0402219].
- [17] T. Bhattacharya, A. Gocksch, C. Korthals Altes and R. D. Pisarski, Phys. Rev. Lett. **66**, 998 (1991); Nucl. Phys. B **383**, 497 (1992) [arXiv:hep-ph/9205231]; S. Chapman, Phys. Rev. D **50**, 5308 (1994) [arXiv:hep-ph/9407313]; J. Wirstam, Phys. Rev. D **65**, 014020 (2002) [arXiv:hep-ph/0106141]; D. Diakonov and M. Oswald, Phys. Rev. D **68**, 025012 (2003) [arXiv:hep-ph/0303129]; [arXiv:hep-ph/0312126]; [arXiv:hep-ph/0403108]; E. Megias, E. Ruiz Arriola and L. L. Salcedo, [arXiv:hep-ph/0312133].
- [18] R. D. Pisarski, Phys. Rev. D **62**, 111501 (2000) [arXiv:hep-ph/0006205].
- [19] A. Dumitru and R. D. Pisarski, Phys. Lett. B **504**, 282 (2001) [arXiv:hep-ph/0010083].
- [20] A. Dumitru and R. D. Pisarski, Phys. Lett. B **525**, 95 (2002) [arXiv:hep-ph/0106176]; Phys. Rev. D **66**, 096003 (2002) [arXiv:hep-ph/0204223]. A. Dumitru, O. Scavenius, and A. D. Jackson, Phys. Rev. Lett. **87**, 182302 (2001) [arXiv:hep-ph/0103219]; O. Scavenius, A. Dumitru and J. T. Lenaghan, Phys. Rev. C **66**, 034903 (2002) [arXiv:hep-ph/0201079]; P. N. Meisinger, T. R. Miller, and M. C. Ogilvie, Phys. Rev. D **65**, 034009 (2002) [arXiv:hep-ph/0108009]; I. I. Kogan, A. Kovner and J. G. Milhano, Jour. High Energy Phys. **0212**, 017 (2002) [arXiv:hep-ph/0208053]; P. N. Meisinger and M. C. Ogilvie, *ibid.* **65**, 056013 (2002) [arXiv:hep-ph/0108026]; K. Fukushima, *ibid.* **68**, 045004 (2003) [arXiv:hep-ph/0303225]; [arXiv:hep-ph/0310121]; Y. Hatta and K. Fukushima, [arXiv:hep-ph/0307068]; [arXiv:hep-ph/0311267].
- [21] R. D. Pisarski, [arXiv:hep-ph/0203271], and references therein.
- [22] A. Mocsy, F. Sannino and K. Tuominen, Phys. Rev. Lett. **91**, 092004 (2003) [arXiv:hep-ph/0301229]; Jour. High Energy Phys. **0403**, 044 (2004) [arXiv:hep-ph/0306069]; [arXiv:hep-ph/0308135]; F. Sannino and K. Tuominen, [arXiv:hep-ph/0403175].
- [23] F. Lenz and M. Thies, Annals Phys. **268**, 308 (1998) [arXiv:hep-th/9802066]; K. Fukushima and K. Ohta, Jour. Phys. G **26**, 1397 (2000) [arXiv:hep-ph/0011108]; L. Dittmann, T. Heinzl and A. Wipf, [arXiv:hep-lat/0306032].
- [24] F. Karsch, E. Laermann and A. Peikert, Phys. Lett. B **478**, 447 (2000) [arXiv:hep-lat/0002003]; Nucl. Phys. B **605**, 579 (2001) [arXiv:hep-lat/0012023].
- [25] O. Kaczmarek, F. Karsch, E. Laermann, and M. Lutgemeier, Phys. Rev. D **62**, 034021 (2000) [arXiv:hep-lat/9908010].
- [26] G. G. Batrouni and B. Svetitsky, Phys. Rev. Lett. **52**, 2205 (1984); A. Gocksch and M. Okawa, *ibid.* **52**, 1751 (1984); J. F. Wheeler and M. Gross, Phys. Lett. B **144**, 409 (1984); Nucl. Phys. B **240**, 253 (1984); S. Ohta and M. Wingate, Phys. Rev. D **63**, 094502 (2001) [arXiv:hep-lat/0006016]; R. V. Gavai, [arXiv:hep-lat/0110054].
- [27] B. Lucini, M. Teper, and U. Wenger, Phys. Lett. B **545**, 197 (2002) [arXiv:hep-lat/0206029]; Jour. High Energy Phys. **0401**, 061 (2004) [arXiv:hep-lat/0307017].
- [28] M. Luscher, [arXiv:hep-lat/9802029]; M. Guagnelli, R. Sommer and H. Wittig, Nucl. Phys. B **535**, 389 (1998) [arXiv:hep-lat/9806005].
- [29] O. Philipsen and H. Wittig, Phys. Rev. Lett. **81**, 4056 (1998) [Erratum-*ibid.* **83**, 2684 (1999)] [arXiv:hep-lat/9807020]; Phys. Lett. B **451**, 146 (1999) [arXiv:hep-lat/9902003]. C. DeTar, O. Kaczmarek, F. Karsch

- and E. Laermann, Phys. Rev. D **59**, 031501 (1999) [arXiv:hep-lat/9808028]; S. Kratochvila and P. de Forcrand, Nucl. Phys. B **671**, 103 (2003) [arXiv:hep-lat/0306011].
- [30] E. Laermann and O. Philipsen, [arXiv:hep-ph/0303042]; F. Karsch and E. Laermann, [arXiv:hep-lat/0305025].
- [31] J.-L. Gervais and A. Neveu, Nucl. Phys. B **163**, 189 (1980).
- [32] A. M. Polyakov, Nucl. Phys. B **164**, 171 (1980).
- [33] V. S. Dotsenko and S. N. Vergeles, Nucl. Phys. B **169**, 527 (1980).
- [34] I. Y. Arefeva, Phys. Lett. B **93**, 347 (1980).
- [35] R. A. Brandt, F. Neri, and M. Sato, Phys. Rev. D **24**, 879 (1981); R. A. Brandt, A. Gocksch, F. Neri, and M. Sato, *ibid.* **26**, 3611 (1982);
- [36] S.V. Ivanov, G.P. Korchemsky, A.V. Radyushkin, Sov. Jour. Nucl. Phys. **44**, 145 (1986); G.P. Korchemsky, A.V. Radyushkin, Phys. Lett. B **279**, 359 (1992); G.P. Korchemsky, A.V. Radyushkin, Nucl. Phys. B **283**, 342 (1987); A. V. Belitsky, A. S. Gorsky and G. P. Korchemsky, Nucl. Phys. B **667**, 3 (2003) [arXiv:hep-th/0304028].
- [37] U. M. Heller and F. Karsch, Nucl. Phys. B **251**, 254 (1985) G. Curci, P. Menotti, G. Paffuti, Z. Phys. C **26**, 549 (1985); H. Markum, M. Faber and M. Meinhardt, Phys. Rev. D **36**, 632 (1987); K. Enqvist, K. Kajantie, L. Karkkainen, and K. Rummukainen, Phys. Lett. B **249**, 107 (1990); J. Kiskis, Phys. Rev. D **41**, 3204 (1990); J. Kiskis and P. Vranas, *ibid.* **49**, 528 (1994); C. P. Korthals Altes, Nucl. Phys. B **420**, 637 (1994) [arXiv:hep-th/9310195].
- [38] J. Zinn-Justin, "Quantum Field Theory and Critical Phenomena" (Clarendon Press, Oxford, 1997).
- [39] O. Kaczmarek, F. Karsch, P. Petreczky, and F. Zantow, Phys. Lett. B **543**, 41 (2002) [arXiv:hep-lat/0207002]; S. Digal, S. Fortunato, and P. Petreczky, [arXiv:hep-lat/0211029]; O. Kaczmarek, F. Karsch, P. Petreczky and F. Zantow, Nucl. Phys. Proc. Suppl. B **129**, 560 (2004) [arXiv:hep-lat/0309121]; O. Kaczmarek, S. Ejiri, F. Karsch, E. Laermann and F. Zantow, [arXiv:hep-lat/0312015]; P. Petreczky and K. Petrov, [arXiv:hep-lat/0405009].
- [40] Yu. M. Makeenko and A. A. Migdal, Phys. Lett. B **212**, 221 (1980); A. A. Migdal, Phys. Rep. **102**, 199 (1983).
- [41] T. Eguchi and H. Kawai, Phys. Rev. Lett. **48**, 1063 (1982); with $p_- = 0$, our (6) is their (18).
- [42] A. Gocksch and F. Neri, Phys. Rev. Lett. **50**, 1099 (1983); R. Narayanan and H. Neuberger, [arXiv:hep-lat/0303023].
- [43] D. J. Gross and E. Witten, Phys. Rev. D **21**, 446 (1980).
- [44] I. Bars, Jour. Math. Phys. **21**, 2678 (1980); S. Samuel, *ibid.* **21**, 2695 (1980); Y. Y. Goldschmidt, *ibid.* **21**, 1842 (1980).
- [45] T. L. Chen, C. I. Tan and X. T. Zheng, Phys. Lett. B **109**, 383 (1982); *ibid.* **123**, 423 (1983); S. Samuel, *ibid.* **112**, 237 (1982); *ibid.* **122**, 287 (1983); Y. M. Makeenko and M. I. Polikarpov, Nucl. Phys. B **205**, 386 (1982); T. L. Chen and Z. Xi-Te, Phys. Rev. D **28**, 3141 (1983);
- [46] P. Menotti and E. Onofri, Nucl. Phys. B **190**, 288 (1981); C. B. Lang, P. Salomonson and B. S. Skagerstam, *ibid.* **190**, 337 (1981); J. P. Rodrigues, Phys. Rev. D **26**, 2833 (1982); S. Samuel, Nucl. Phys. B **205**, 221 (1982); M. C. Ogilvie and A. Horowitz, Nucl. Phys. B **215**, 249 (1983); J. Jurkiewicz and K. Zalewski, Nucl. Phys. B **220**, 167 (1983); J. Jurkiewicz, C. P. Korthals Altes and J. W. Dash, Nucl. Phys. B **233**, 457 (1984); J. Jurkiewicz and C. P. Korthals Altes, Nucl. Phys. B **242**, 62 (1984).
- [47] J. B. Kogut, M. Snow, and M. Stone, Nucl. Phys. B **200**, 211 (1982).
- [48] J. Polonyi and K. Szlachanyi, Phys. Lett. B **110**, 395 (1982); J. Bartholomew, D. Hochberg, P. H. Damgaard, and M. Gross, *ibid.* **133**, 218 (1983); M. Gross and J. F. Wheeler, Nucl. Phys. B **240**, 253 (1984); A. Gocksch and M. Ogilvie, Phys. Rev. D **31**, 877 (1985); P. H. Damgaard and A. Patkos, Phys. Lett. B **172**, 369 (1986); C. X. Chen and C. DeTar, Phys. Rev. D **35**, 3963 (1987); M. Ogilvie, Phys. Rev. Lett. **52**, 1369 (1987).
- [49] F. Green and F. Karsch, Nucl. Phys. B **238**, 297 (1984).
- [50] J. Gasser and H. Leutwyler, Phys. Lett. B **188**, 477 (1987); H. Leutwyler and A. Smilga, Phys. Rev. D **46**, 5607 (1992); recent work includes: G. Ake-
mann, J. T. Lenaghan and K. Splittorff, Phys. Rev. D **65**, 085015 (2002) [arXiv:hep-th/0110157]; J. Lenaghan and T. Wilke, Nucl. Phys. B **624**, 253 (2002); P. H. Damgaard, M. C. Diamantini, P. Hernandez and K. Jansen, Nucl. Phys. B **629**, 445 (2002) [arXiv:hep-lat/0112016]; P. H. Damgaard, P. Hernandez, K. Jansen, M. Laine and L. Lellouch, *ibid.* **656**, 226 (2003) [arXiv:hep-lat/0211020].
- [51] J. M. Drouffe and J. B. Zuber, Phys. Rep. **102**, 1 (1983); S. R. Das, Rev. Mod. Phys. **59**, 235 (1987); P. Di Francesco, P. H. Ginsparg and J. Zinn-Justin, Phys. Rep. **254**, 1 (1995) [arXiv:hep-th/9306153]; R. C. Brower, M. Campostrini, K. Orginos, P. Rossi, C. I. Tan and E. Vicari, Phys. Rev. D **53**, 3230 (1996) [arXiv:hep-th/9508015]; P. Rossi, M. Campostrini and E. Vicari, Phys. Rep. **302**, 143 (1998) [arXiv:hep-lat/9609003]; M. Billo, M. Caselle, A. D'Adda and S. Panzeri, Intl. Jour. Mod. Phys. **A12**, 1783 (1997) [arXiv:hep-th/9610144]; Yu. Makeenko, [arXiv:hep-th/0001047]; M. R. Douglas, I. R. Klebanov, D. Kutasov, J. Maldacena, E. Martinec and N. Seiberg, [arXiv:hep-th/0307195].
- [52] D. J. Gross and W. I. Taylor, Nucl. Phys. B **400**, 181 (1993) [arXiv:hep-th/9301068]; *ibid.* **403**, 395 (1993) [arXiv:hep-th/9303046].
- [53] P. Cvitanovic, <http://www.nbi.dk/GroupTheory>; H. Elvang, P. Cvitanovic and A. D. Kennedy, [arXiv:hep-th/0307186].
- [54] P. H. Damgaard, Phys. Lett. B **194**, 107 (1987).
- [55] A. Dumitru, J. Lenaghan, R. D. Pisarski, and K. Splittorff, work in progress.
- [56] K. Redlich, H. Satz and J. Seixas, Phys. Lett. B **208**, 291 (1988); K. Redlich and H. Satz, *ibid.* **213**, 191 (1988); J. Engels, J. Fingberg, K. Redlich, H. Satz and M. Weber, Z. Phys. C **42**, 341 (1989); J. Fingberg, D. E. Miller, K. Redlich, J. Seixas and M. Weber, Phys. Lett. B **248**, 347 (1990); J. Christensen and P. H. Damgaard, Nucl. Phys. B **348**, 226 (1991); J. Engels and V. K. Mitrjushkin, Phys. Lett. B **282**, 415 (1992); P. H. Damgaard and M. Hasenbusch, Phys. Lett. B **331**, 400 (1994) [arXiv:hep-lat/9404008]; J. Engels, F. Karsch, and K. Redlich, Nucl. Phys. B **435**, 295 (1995) [arXiv:hep-lat/9408009]; J. Engels, S. Mashkevich, T. Scheideler, and G. Zinovev, Phys. Lett. B **365**, 219 (1996) [arXiv:hep-lat/9509091]; J. Engels and T. Scheideler, *ibid.* **394**, 147 (1997) [arXiv:hep-lat/9610019]; Nucl. Phys. B **539**, 557 (1999) [arXiv:hep-lat/9808057].
- [57] M. Albanese *et al.* [APE Collaboration], Phys. Lett. B

- 192**, 163 (1987); C. Morningstar and M. J. Peardon, Phys. Rev. D **69**, 054501 (2004) [arXiv:hep-lat/0311018].
- [58] There is no deconfining transition in two spacetime dimensions. Gauge theories have no dynamical degrees of freedom, and all Wilson lines can be computed from free field theory: G. Grignani, G. W. Semenoff and P. Sodano, [arXiv:hep-th/9503109]; L. D. Paniak, G. W. Semenoff and A. R. Zhitnitsky, Nucl. Phys. B **506**, 521 (1997) [arXiv:hep-ph/9701270]; U. G. Mitreuter, J. M. Pawłowski and A. Wipf, *ibid.* **514**, 381 (1998) [arXiv:hep-th/9611105]; G. Grignani, L. Paniak, G. W. Semenoff and P. Sodano, Annals Phys. **260**, 275 (1997) [arXiv:hep-th/9705102]; J. M. Aroca and Y. Kubyshin, *ibid.* **283**, 11 (2000) [arXiv:hep-th/9901155].
- [59] S. Mandelstam, Phys. Rev. D **19**, 2931 (1979).
- [60] J. Papavassiliou and R. D. Pisarski, work in progress.
- [61] If $\beta_N = 0$, couplings for the two-index tensor, and adjoint, representations, must be included, $\beta_{N(N\pm 1)/2}$ and β_{N^2-1} , respectively. (For $N \geq 4$, both symmetric and anti-symmetric two-index tensor representations enter, with corrections to factorization $\sim 1/N$.) The case where the couplings for $Z(N)$ charged fields vanish, $\beta_N = \beta_{N(N\pm 1)/2} = 0$, but that for the $Z(N)$ neutral field(s) do not, such as $\beta_{N^2-1} \neq 0$, is special. In this case, the global $Z(N)$ symmetry is promoted to a local symmetry, and while $Z(N)$ neutral fields can condense above some temperature, loops with nonzero $Z(N)$ charge cannot at $N < \infty$. We assume this doesn't happen: that $\beta_N \neq 0$, and other couplings are small corrections.
- [62] These two string tensions can be computed in the Nambu string model by expanding in a large number of space-time dimensions, d . The ordinary string tension, $\sigma(T)$, is computed from the two point function of Polyakov loops; it corresponds to a surface in which the transverse fluctuations are tied down on two sides, with free boundary conditions in imaginary time at $\tau = 0, 1/T$: O. Alvarez and R. D. Pisarski, Phys. Rev. D **26**, 3735 (1982). The loop string tension, $\sigma_{loop}(T)$, corresponds to a surface tied down on four sides, setting the transverse fluctuations to vanish at $\tau = 0, 1/T$. This follows from the potential at zero temperature, O. Alvarez, Phys. Rev. D **24**, 440 (1981), by replacing $R \leftrightarrow 1/T$. These two string tensions agree at $T = 0$, but differ at $T \neq 0$. In a large d expansion,
- $$\frac{\sigma(T)}{\sigma_0} = \sqrt{1 - \left(\frac{T}{T_d}\right)^2}, \quad \frac{\sigma_{loop}(T)}{\sigma_0} = \sqrt{1 - \left(\frac{T}{2T_d}\right)^2},$$
- where $T_d^2 = 3\sigma_0/(\pi d)$, and σ_0 is the string tension at zero temperature. Surfaces for the loop string tension fluctuate less, so while σ vanishes at T_d , σ_{loop} doesn't vanish until $2T_d$, and $\sigma_{loop}(T_d)/\sigma_0 = \sqrt{3}/2 \approx .87$.
- [63] The flatness of \mathcal{V}_{mf} at $\beta = 1$ was noted by [47] and [49], but dismissed as unphysical. At the time, however, neither the decrease in the string tension near T_d , nor the weakness of the first order transition, were seen in numerical simulations [25].
- [64] E. Witten, Nucl. Phys. B **145**, 110 (1978).
- [65] K. Holland, P. Minkowski, M. Pepe and U. J. Wiese, Nucl. Phys. B **668**, 207 (2003) [arXiv:hep-lat/0302023].
- [66] A. M. Polyakov, Nucl. Phys. Proc. Suppl. B **68**, 1 (1998) [arXiv:hep-th/9711002]; A. M. Polyakov and V. S. Rychkov, Nucl. Phys. B **581**, 116 (2000) [arXiv:hep-th/0002106].

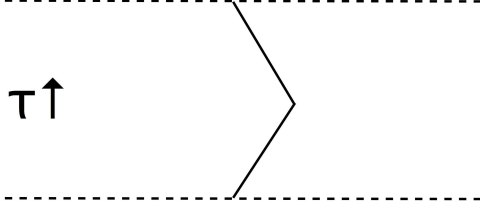


FIG. 1: A Polyakov loop with two cusps, at $\tau = 0$ and $\tau = 1/(2T)$. The dotted lines denote $\tau = 0$ and $1/T$.

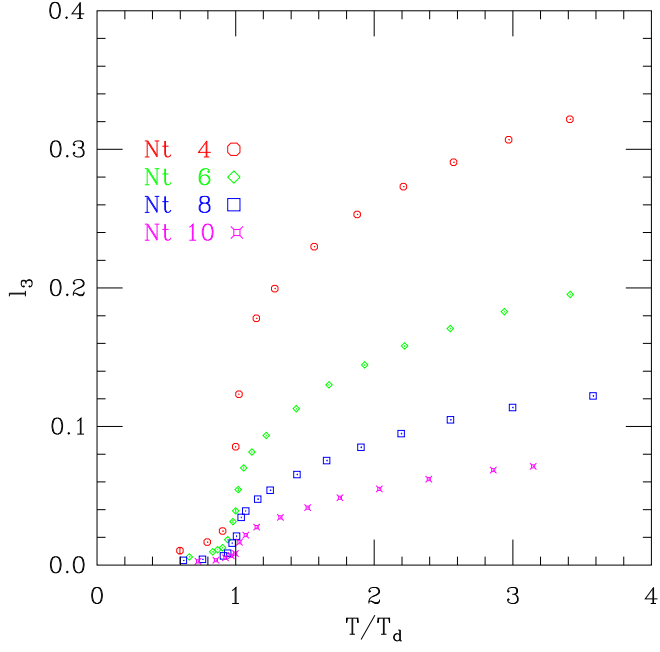


FIG. 2: The bare triplet Polyakov loop as a function of temperature.

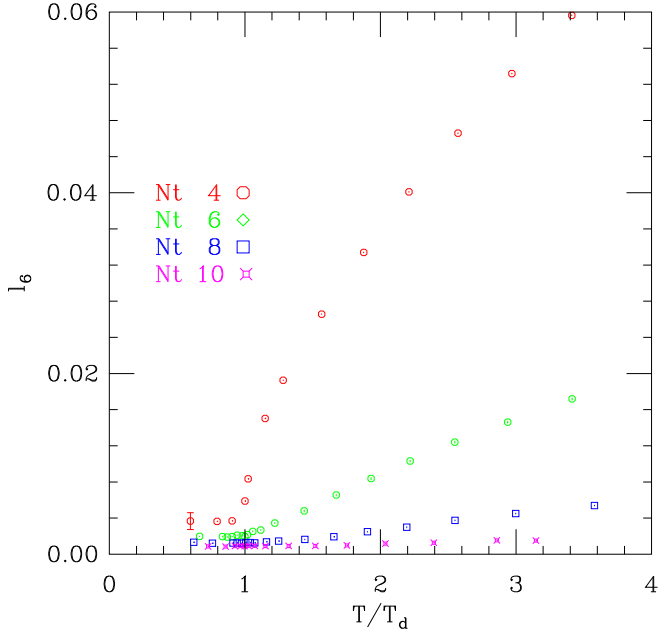


FIG. 3: The bare sextet Polyakov loop as a function of temperature.

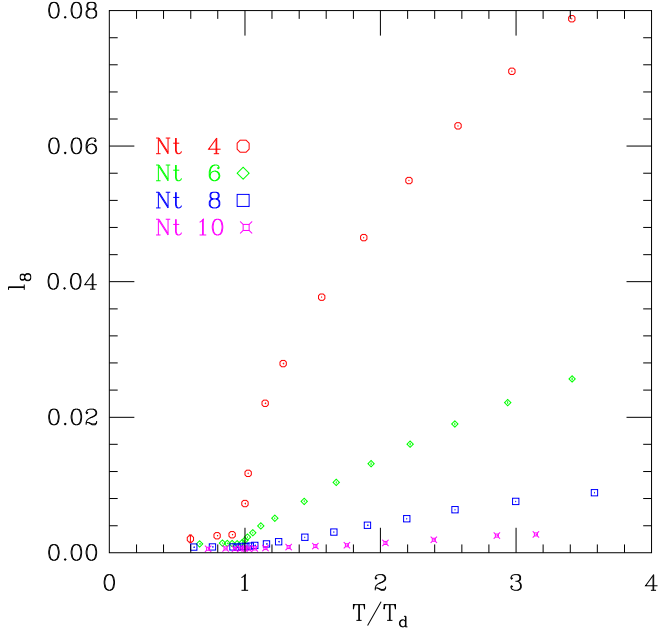


FIG. 4: The bare adjoint Polyakov loop as a function of temperature.

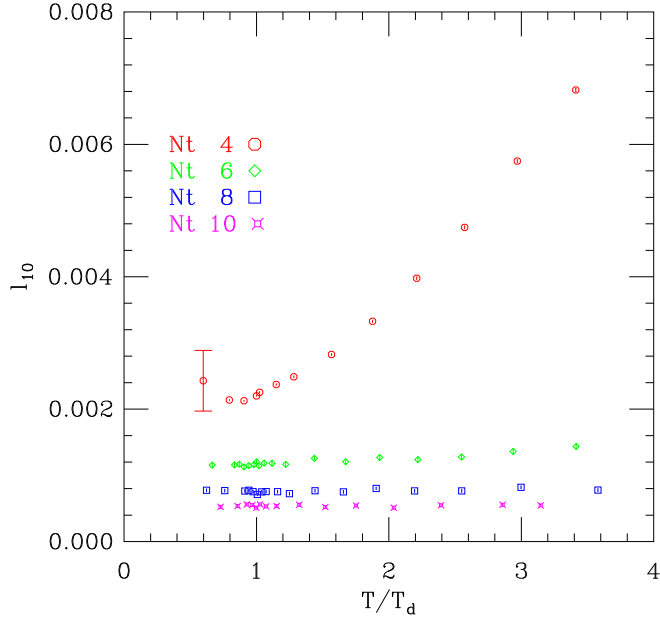


FIG. 5: The bare decuplet Polyakov loop as a function of temperature.

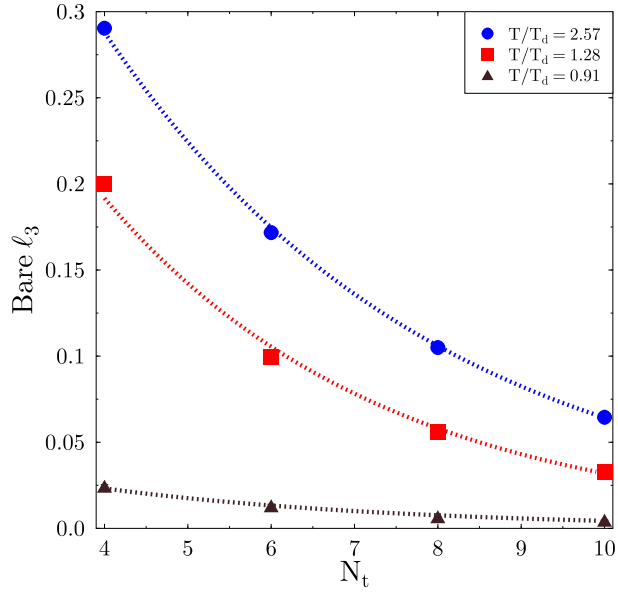


FIG. 6: The bare triplet Polyakov loop at fixed temperature, as a function of N_t .

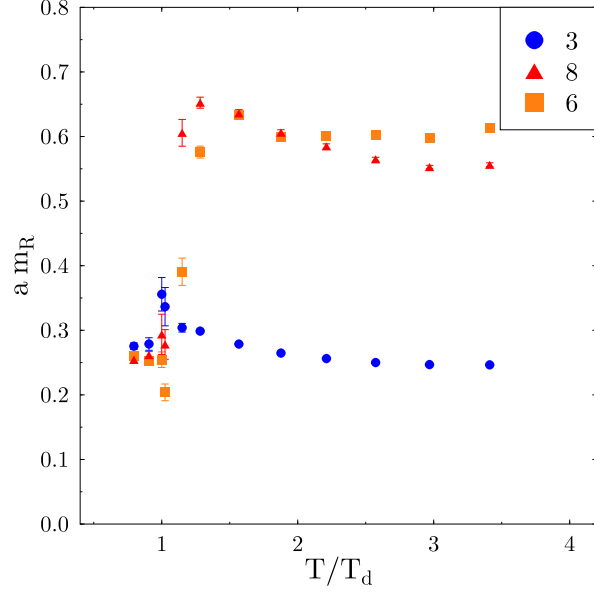


FIG. 7: The divergent masses, times lattice spacing, versus temperature.

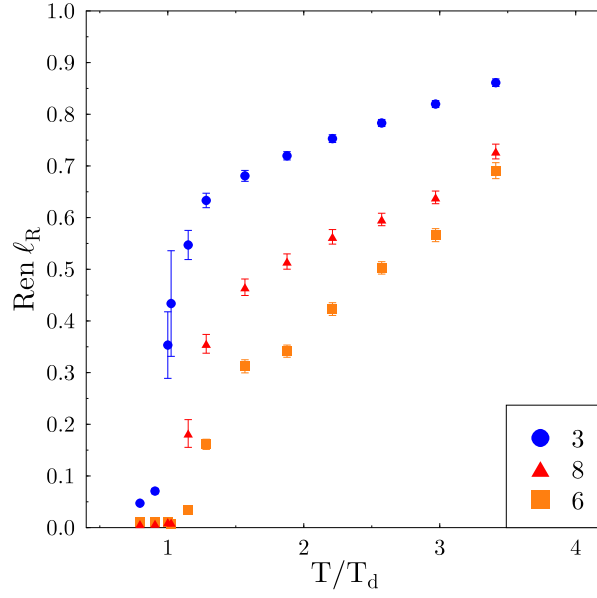


FIG. 8: Renormalized Polyakov loops as a function of temperature.

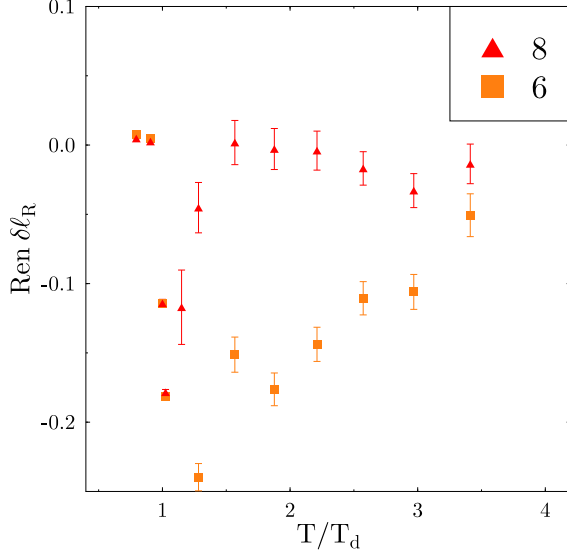


FIG. 9: Difference loops: renormalized Polyakov loops, minus their large N values.

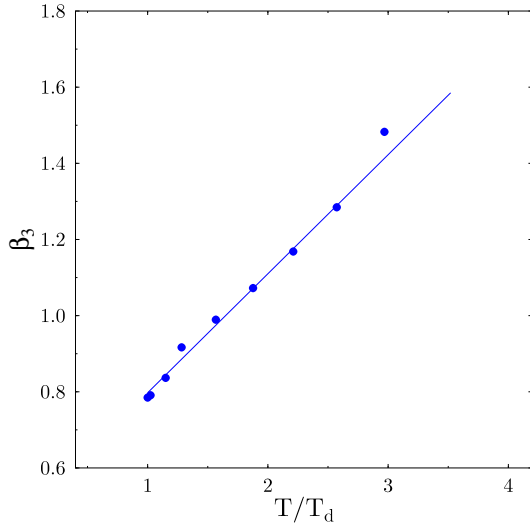


FIG. 10: The fundamental coupling constant extracted from the lattice data. The circles are the fundamental coupling computed from lattice data for the fundamental loop. The error bars on the extracted points are smaller than data points. The smooth line is the linear fit to the extracted fundamental coupling with the errors quoted in (71).

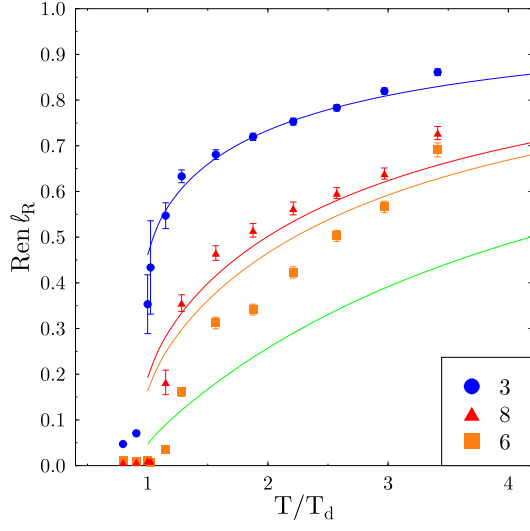


FIG. 11: The values of the Polyakov loops from the matrix model, using the linear relationship between the coupling and the temperature. The lower-most (green) line corresponds to the value of the decuplet loop, for which there is no lattice data.

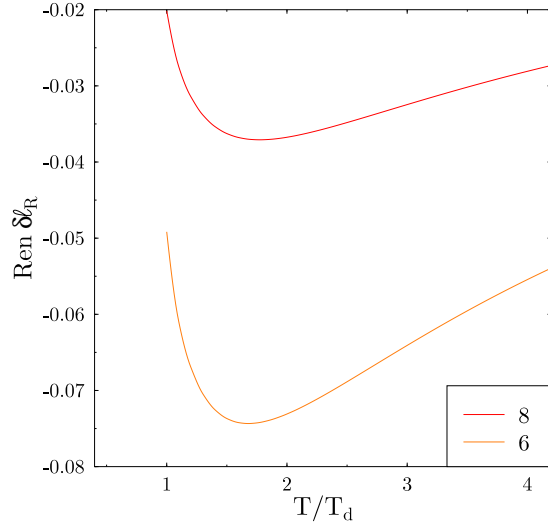


FIG. 12: Difference loops from the matrix model: Polyakov loops, minus their large N values.